



**HAL**  
open science

# Revising dating estimates and the antiquity of eusociality in termites using the fossilized birth-death process

Corentin Jouault, Frédéric Legendre, Philippe Grandcolas, André Nel

## ► To cite this version:

Corentin Jouault, Frédéric Legendre, Philippe Grandcolas, André Nel. Revising dating estimates and the antiquity of eusociality in termites using the fossilized birth-death process. *Systematic Entomology*, 2021, 46 (3), pp.592-610. 10.1111/syen.12477 . insu-03188488

**HAL Id: insu-03188488**

**<https://insu.hal.science/insu-03188488>**

Submitted on 2 Apr 2021

**HAL** is a multi-disciplinary open access archive for the deposit and dissemination of scientific research documents, whether they are published or not. The documents may come from teaching and research institutions in France or abroad, or from public or private research centers.

L'archive ouverte pluridisciplinaire **HAL**, est destinée au dépôt et à la diffusion de documents scientifiques de niveau recherche, publiés ou non, émanant des établissements d'enseignement et de recherche français ou étrangers, des laboratoires publics ou privés.

Revising dating estimates and the antiquity of eusociality in termites using the fossilized birth-death process

CORENTIN JOUAULT\*,<sup>1</sup>, FREDERIC LEGENDRE<sup>2</sup>, PHILIPPE GRANDCOLAS<sup>2</sup> and ANDRE NEL\*,<sup>2</sup>

<sup>1</sup>Univ. Rennes, CNRS, Geosciences Rennes, UMR 6118, F-35000, Rennes, France.

<sup>2</sup>Institut de Systématique, Évolution, Biodiversité (ISYEB) Muséum national d'Histoire naturelle, CNRS, Sorbonne Université, EPHE, Université des Antilles, CP50, 57 rue Cuvier 75005 Paris, France. E-mails: frederic.legendre@mnhn.fr, orcid.org/0000-0001-5900-8048; pg@mnhn.fr, orcid.org/0000-0003-1374-1222; anel@mnhn.fr, orcid.org/0000-0002-4241-7651

\* Correspondence:

Corentin Jouault, Univ. Rennes, CNRS, Geosciences Rennes, UMR 6118, F-35000, Rennes, France.

E-mail: jouaultc0@gmail.com, orcid.org/0000-0002-3680-5172

&

André Nel, Institut de Systématique, Évolution, Biodiversité (ISYEB) Muséum national d'Histoire naturelle, CNRS, Sorbonne Université, EPHE, Université des Antilles, CP50, 57 rue Cuvier 75005 Paris, France. E-mail: anel@mnhn.fr, orcid.org/0000-0002-4241-7651

**Running title.** Revising antiquity of termite eusociality

**Keywords.** Time divergence, FBD, tip-dating, morphological phylogeny, Cretaceous, calibration, ghost lineages

**Abstract.** Deciphering the timing and tempo of lineage diversification of organisms has greatly benefited from advances in Bayesian phylogenetic analyses using morphological data. Those advances, however, have not been used for termites despite a rich fossil record. Here, we estimate divergence times for living and fossil termites using the fossilized birth–death (FBD) process on a previously published morphological matrix expanded with two new fossils that we describe (see Appendices 1 & 2). Those fossils, based on soldier specimens, are the ‘mid’-Cretaceous mastotermitid *Milesitermes engeli* **gen. et sp. nov.**, and the Middle Eocene *Reticulitermes grimaldii* **sp. nov.** The latter is the oldest occurrence of a Rhinotermitidae soldier and the first termite soldier described from Baltic amber. Our dating estimates provide new stem- and crown-ages for termites, suggesting older ages than previously thought for several lineages. Importantly, crown-Isoptera—and therefore eusociality—may have arisen ~200 Ma. We conclude with further directions to keep improving our understanding of the timing of differentiation in termites.

## Introduction

Deciphering the timing and tempo of lineage diversification of organisms has greatly benefited from advances in Bayesian phylogenetic analyses using morphological data, allowing to include fossil taxa in tip-dating or total-evidence analyses (dos Reis *et al.*, 2016; Wright, 2019). Even if some methodological refinements are still under development (e.g. Keating *et al.*, 2020), those analyses have shed insights on the evolution of organisms, sometimes resulting in a better fit with stratigraphic evidence (King, 2020), sometimes clarifying the tempo of diversification of several lineages with a robust fossil record such as mammals (King and Beck, 2020), Mesozoic birds (Zhang & Wang, 2019), Lissamphibia (Pyron, 2011), and Hymenoptera (Ronquist *et al.*, 2012). Despite several remarkable fossils—including two new species based on soldier specimens that we describe here—the timing of the evolution of termites and their eusocial system has never been investigated with those latest developments.

The spectacular evolutionary and ecological success of termites is mostly attributed to their highly integrated eusocial system, defined by cooperative brood care, overlapping generations within a colony, and the division of labor into reproductive and non-reproductive castes (Wilson, 1971, 1975; Lin & Michener, 1972; Wilson & Hölldobler, 2005). Termites are regarded as the first animals that have evolved eusociality (Grimaldi & Engel, 2005; Legendre & Condamine, 2018; Barden & Engel, 2020; Zhao *et al.* 2020b) because they show the oldest record of morphologically specialized soldiers (Engel *et al.*, 2016; Zhao *et al.*, 2019, 2020a), although the discovery of Cretaceous ant fossils has questioned this assertion (Perrichot, 2019). Clarifying the timing of diversification of termites is also critical to understand the underlying roles of environmental factors in the evolution of highly integrated social systems (Grandcolas & D’Haese, 2002; Legendre *et al.*, 2008, 2013, 2015).

Most molecular phylogenies have agreed on a termite crown-age dating back to ca. 150 Ma (e.g. Bourguignon *et al.*, 2015; Legendre *et al.*, 2015). Nevertheless, discrepancies exist among dating estimates for this group and its families (Evangelista *et al.*, 2019), whether estimated from molecular or morphological evidence. Some of the most recent phylogenetic analyses have relied on molecular

data, using fossils as node calibrations only (Bourguignon *et al.*, 2015; Legendre *et al.*, 2015; Wu *et al.*, 2018; Bucek *et al.*, 2019; Condamine *et al.*, 2020). Others have used morphological data with fossils as terminals, but the phylogenies were built in a parsimony framework, wherein crown- and stem-ages of termite families were educated guesses (Engel *et al.*, 2009; Krishna *et al.*, 2013; Zhao *et al.*, 2019, 2020a). A single study (Ware *et al.*, 2010) used extant and fossil taxa as terminals in a Bayesian framework; it was conducted, however, before significant methodological improvements in tip-dating analyses were developed (e.g. Heath *et al.*, 2014). Those different practices led to different results, sometimes tens of Myrs apart in their mean estimates. To obfuscate things even further, some ichnofossils, namely Triassic, Early and Late Jurassic putative nests, are controversial. Sometimes regarded as evidence of a Triassic, or even earlier origin of termites (Hasiotis & Dubiel, 1995; Bordy *et al.*, 2004, 2009, 2010; Smith *et al.*, 2020), the oldest ones are judged by others as lacking proper analyses to form conclusive evidence of Triassic antiquity of termites (Genise *et al.*, 2005; Genise, 2016). To our knowledge, however, they have never been used to calibrate phylogenetic trees.

In order to clarify the timing of the origin of termites and their constitutive extant and extinct families, we first expand the termite fossil record by describing two new species from soldier specimens. Next, we take advantage of the fossilized birth–death (FBD) model (Heath *et al.*, 2014) and of a previous morphological dataset (Engel *et al.*, 2009, 2016; Zhao *et al.*, 2019) to estimate datings that we contrast with estimates from a node-dating analysis and from previous works. We then discuss those estimates and their implications, including the origin of termite eusociality.

## **Materials and methods**

### *Origin, preparation and examination of amber pieces*

The amber pieces containing the specimens studied herein come from the two main amber deposits of the world (Grimaldi *et al.*, 2002; Weitschat & Wichard, 2010), respectively Burmese and Baltic amber.

One is embedded in a piece of yellow Burmese amber with numerous debris. This amber comes from Noiye Bum in the Hukawng Valley (26° 29' N, 96° 35' E), Kachin State, northern Myanmar (see detailed map in Grimaldi and Ross, 2017: fig. 2). Taphonomic analyses of pholadids and radiometric data, based on zircons from volcanic clasts found within the amber-bearing sediments, established an early Cenomanian age ( $98.79 \pm 0.62$  Ma) for Kachin amber (Shi *et al.*, 2012; Smith & Ross, 2017). Some ammonites found in the amber-bearing bed and within amber corroborate a Late Albian / Early Cenomanian age (Cruickshank & Ko, 2003; Yu *et al.*, 2019).

The other is embedded in a piece of clear yellow Baltic amber with at least three Diptera and two Collembola as syninclusions. This amber comes from the Blue Earth Formation (or Blue Earth member of the Prussian Formation) from the Kaliningrad Russian enclave (54°41'19.5"N, 20°20'50.6"E). Blue Earth Formation was dated as late Bartonian to Priabonian (Upper Eocene, ca. 34–38 Ma) based on palynological data (Kosmoswska-Ceranowicz *et al.*, 1997; Aleksandrova & Zaporozhets, 2008). Discussions on the age and paleobiota of Baltic amber can be found in Weitschat & Wichard (2010), Sadowski *et al.* (2017), and Alekseev (2018).

The amber pieces were polished with a grinder polisher (Buehler EcoMet 30) by using a very thin silicon carbide sanding paper (grit size = 7000). Then, the fragment was embedded with cedar oil between microscopic slides to minimize light scattering during focus stacking.

Both specimens are housed in the amber collection of the Geological Department and Museum (IGR) of the University of Rennes (France), respectively under the collection number IGR.BU-012 and IGR.BA-020. Amber pieces and specimens were examined with a Leica MZ APO stereomicroscope, and a Nikon SMZ25 stereomicroscope. Photographs were taken using a Canon EOS 5D mark II mounted on a Leica MZ APO stereomicroscope. All images are digitally stacked photomicrographic composites of several individual focal planes, obtained using HeliconFocus 6.7 software. Figures were composed with Adobe Illustrator CC 2019 and Photoshop CC 2019 software. We follow the morphological terminology and the classification of termites as presented in Krishna *et al.* (2013), and thus retain the rank Isoptera.

### *Morphological dataset*

Phylogenetic analyses were conducted to i) clarify the phylogenetic positions of the two new genera described herein, and ii) estimate divergence times for termites and their subgroups. The morphological matrix (Appendix 1) was modified from Engel *et al.* (2016) with insightful corrections from Zhao *et al.* (2019). The data set is composed of 111 morphological characters (Appendix 2) coded for 89 extant and extinct taxa. The outgroup comprises four cockroaches and one mantid (*Chaeteessa* sp., *Panchlora* sp., *Periplaneta americana*, *Cryptocercus* sp. 1, and *Cryptocercus* sp. 2). The ingroup has representatives for all extant and extinct families. The morphological matrix was established using Mesquite software ver. 3.61 (Maddison & Maddison, 2019), with all characters unordered, non-polarized, and of equal weight. Characters coded as inapplicable were treated as missing data and coded ‘-’, while unknown characters were coded ‘?’. Missing data and unknown characters represent respectively 8.57 % and 22.13 % of the dataset. All consensus trees were visualized and drawn using FigTree ver. 1.4.4 (Rambaut, 2009), and modified with Adobe Illustrator CC2019.

### *Tree reconstruction and dating estimates in Bayesian inference*

We performed two kinds of analyses using relaxed clock models in MrBayes 3.2.7a (Huelsenbeck & Ronquist, 2001; Ronquist & Huelsenbeck, 2003; Ronquist *et al.*, 2012). First, we computed node-dating analyses with only extant taxa, fossils being used to calibrate nodes (see below for justifications of fossil calibrations). Second, we computed tip-dating analyses with a fossilized birth-death model (FBD; Heath *et al.*, 2014) wherein fossil taxa are terminals. Because not all the expected inter-familial relationships were found in unconstrained analyses—an unsurprising outcome for a relatively small dataset comprising only morphological characters (see Supporting Information)—and because our aim is not to reassess phylogenetic relationships but rather age estimates, we added four topology constraints (i.e. monophyly of Blattodea, (*Cryptocercus* +

Isoptera), Isoptera, and Neoisoptera but Stylotermitidae). Those constraints fit the current understanding in termite phylogenetics (notably Wu *et al.*, 2018 for Stylotermitidae), thus ensuring better estimates of the parameters under investigation (i.e. ages; Zhang & Wang, 2019; Luo *et al.*, 2020).

All but one analyses were computed with a Mkv model (Lewis, 2001) with a gamma rate variation across characters and with the independent gamma relaxed clock model (Lepage *et al.*, 2007; *lset rates = invgamma, prset clockvarpr = igr, prset igrvarpr = exp(10)*); the exception was computed with no rate variation across characters: *lset rates = equal*). The prior used for the mean clock rate was gamma (2, 200), except in one analysis wherein we tested a normal but very flat prior (*prset clockratepr = normal(0.0025,1)*) and a flat uniform speciation prior (*prset speciationpr = uniform(0,10)*; Matzke & Wright, 2016). The proportion of extant taxa was set to 0.012 (37 termite terminals for ca. 3000 species; *prset sampleprob=0.012*). Sampling strategy of taxa was either set to diversity (*prset samplestrat=diversity* wherein fossils are sampled randomly and can be tips or ancestors), random (*prset samplestrat=random* wherein fossils can be tips or ancestors) or fossiltip (*prset samplestrat=fossiltip* wherein fossil and extant taxa are assumed to be sampled randomly and fossil ancestor is not allowed). An exponential prior and a beta prior were used for the net speciation rate and the relative extinction rate, respectively [*prset speciationpr = exp(100)*; *prset extinctionpr = beta(1,1)*], while the node age prior was set to ‘calibrated’. All analyses comprised two runs and four chains, and were launched for 50 million generations. Chains were sampled every 5000 generations and a burn-in fraction of 0.25 was used. Convergence diagnostics were checked for each analysis [i.e. average standard deviation of split frequencies < 0.01, PRSF close to 1.0, and ESS > 200 in Tracer (Rambaut *et al.*, 2018); see also Supporting Information].

*Node-dating analyses* – These four analyses have a reduced taxonomic sampling comprising only extant taxa (Ntax = 42). The prior probability distribution on branch lengths was either set to *clock:birthdeath* (two analyses) or *clock:uniform* (two analyses). Three nodes were assigned offset exponential priors: the root of the tree (minimum age: 225 Ma, mean age: 270 Ma), Blattodea (150,

225 Ma) and Isoptera (137, 150 Ma). Those ages were set according to the latest studies (Bourguignon *et al.*, 2015, 2018; Legendre *et al.*, 2015; Engel *et al.*, 2016; Bucek *et al.*, 2019; Evangelista *et al.*, 2019; Zhao *et al.*, 2020a; more details in Appendix 3).

*Tip-dating analyses* – For the 13 tip-dating analyses, extinct taxa were calibrated with uniform distributions (Appendix 3) bounded according to the minimum and maximum ages of their deposits (Barido-Sottani *et al.*, 2019; ten analyses) or with fixed distributions bounded according to the minimum ages of their deposits (three analyses). For the fossilized birth-death process, sampling fossil ancestors (Gavryushkina *et al.*, 2014; Zhang *et al.*, 2016) was allowed in four analyses, whereas all fossils were set as tips in the others (*prset samplestrat = fossiltip*). The prior probability distribution on branch lengths was set to *clock:fossilization*, except in a single analysis (*prset brlenspr = clock:uniform*). Because the dataset comprises characters of alates, workers, soldiers, and life history traits, we conducted analyses with and without partitioning of the data (i.e. a single or three partitions; in the latter, alate and worker characters belong to the same partition). Our aim was to check whether data partitioning would affect age estimates, as well as evolutionary rates.

Finally, some analyses were computed, modifying one prior at a time relative to the one partition analysis, to assess the robustness of our results. The modified priors were the mean age of termites MRCA (difference with the minimum age halved or doubled; i.e. 144 or 163 Ma) and a variable partition specific rate prior (i.e. *prset ratepr = variable*).

Overall, 17 tip-dating and node-dating analyses were performed on CIPRES portal with MrBayes 3.2.7a on XSEDE (Miller *et al.*, 2010); all scripts are provided as Supporting Information.

#### *Tree reconstruction in parsimony*

We performed a tree reconstruction using maximum of parsimony (MP) in PAUP ver. 4.0a166 (Swofford, 2002) to compare the topology with the Bayesian inference. The outgroup was treated as paraphyletic with respect to the ingroup, and the tree search was performed using a heuristic search method with the following options: maximum number of trees saved equal to 10000, only optimal

trees retain, collapse of zero-length branches, and a TBR swapping algorithm. The search produced more than one equally parsimonious cladogram so that a strict consensus cladogram was built to summarize the results. Bremer indices were computed (Bremer, 1994), as well as Bootstrap support values (bs) using the heuristic search option for 100 replicates (Felsenstein, 1985; Hillis & Bull, 1993). The consensus cladogram with bs and Bremer indices is provided as a Supplementary file (Suppl. fig. 1).

Published work and nomenclatural acts are registered in ZooBank (<http://www.zoobank.org/>, last access: 20 February 2021), with the following LSID (reference):  
urn:lsid:zoobank.org:pub:D3EBBA6B-F488-4B56-AC98-0418A6B353FC

## Results

### *Systematic Palaeontology*

Order Blattodea, Latreille, 1810

Infraorder Isoptera Brullé, 1832

Epifamily Termitoidae Latreille, 1802

Family Mastotermitidae Desneux, 1904

***Milesitermes* gen. nov.** Jouault & Nel

(Figs 1-2)

urn:lsid:zoobank.org:act:5711364A-9468-4315-A380-23CB17AF96BB

***Etymology:*** The generic epithet is a combination of the Latin word *Miles* meaning ‘soldier’ and *Termes* commonly used to designate Isoptera. The generic epithet refers to the description based on a soldier specimen. Gender masculine.

***Type species:*** *Milesitermes engeli* sp. nov.

**Diagnosis:** Head capsule extended, cylindrical-rectangular shaped. Antenna moniliform. Epicranial suture maybe present. Mandibles stout slightly elongated, and hooked apically, right mandible with one marginal tooth. Pronotum remarkable, trapezoidal, large, as wide as head capsule, anterior margin concave, slightly saddle shape, lateral margin convex, posterior margin nearly straight. Procoxal carina present. Legs with tarsi pentamerous, tibial spur formula 3–4–4, all tibiae with extra spines and rows of macrosetae. Abdomen plump and slightly elongate, and cerci four-segmented.

*Milesitermes engeli* **sp. nov.** Jouault & Nel (Figs 1-2)

urn:lsid:zoobank.org:act:70D5C4CA-3CA2-4E09-98E7-D943E2C909B1

**Holotype:** soldier, accession number IGR.BU-012 (a nearly complete specimen in a rounded piece of amber measuring 5 × 10 × 3 mm with numerous debris and wood fiber).

**Etymology:** The specific epithet is a patronym honoring our colleague Pr. Michael S. Engel, eminent American paleoentomologist, and specialist of Isoptera. The species epithet is to be treated as a noun in the genitive case.

**Locality and horizon:** Noiye Bum Hill, Hukawng Valley, Kachin State, Myanmar; upper Albian to lower Cenomanian, mid-Cretaceous.

**Diagnosis:** As for the genus.

**Description:** Large soldier termite, body length *ca.* 6.40 mm from tip of mandible to apex of abdomen. Head massive, width *ca.* 1.65 mm, length *ca.* 2.35 mm from buccal aperture to posterior margin of head, *ca.* 2.7 mm total (including mandibles); head capsule longer than wide; lateral margins nearly parallel; posterior border touching anterior margin of pronotum. Mandibles strongly sclerotized, clearly prognathous, dentate; left mandible destroyed; right mandible partially preserved, *ca.* 0.82 mm long, greatest exposed width *ca.* 0.28 mm; dentition visible on right mandible only; apex of right mandible slender, pointed and hooked, with one shallow triangular median tooth. Labrum, anteclypeus, postclypeus, and clypeus not preserved. Antennae partially destroyed, with more than six antennomeres (six preserved on left antenna). Compound eye not visible. Posterior part of head

capsule with maybe remains of a faint epicranial ecdysial cleavage scar. Maxillary palps with five palpomeres, basal palpomere shortest, ultimate one longest; maxillary palpomeres length (when measurable) in mm: P5 0.26, P4 0.21, P3 0.2; labial palps with three(?) visible palpomeres, basal palpomere shortest, apical one longest. Paraglossa three(?) -segmented with apical segment the longest and apically rounded. Lacinial incisor conspicuous with one apical tooth and a basal one shorter. Galea visible but poorly preserved, other mouthparts hardly visible. Cervical sclerites massive, two-segmented (an inner cervical sclerite and lateral cervical sclerite on each side). Pronotum massive in contact with head posterior margin, widest than head, trapezoidal shaped with anterior part the widest, anterior margin concave, antero-lateral corners rounded; lateral margins gently convex; posterior margin nearly straight with a small median concavity, postero-lateral corner broadly rounded; pronotal dimensions: median length 0.71 mm; greatest length 0.8 mm; greatest width 1.78 mm (across anterior portion); median portion of pronotum slightly raised longitudinally, two reduced depressions lateral to this raising. Mesonotum and metanotum largely transverse, mesonotal greatest length 0.66 mm, width 1.32 mm; mesonotum trapezoidal shaped with antero- and postero-lateral corners rounded, mesonotum overlapping metanotum. Legs with tarsi wholly pentamerous (i.e., no cryptic tarsomere), tibiae spinose, tibial spines asymmetrical, with finely serrate margin; arolium present between pretarsal claws. Foreleg smallest, procoxa small with carina present, profemora *ca.* 1 mm long, protibia slender, *ca.* 0.7 mm long, protarsus *ca.* 0.3 mm, pretarsal claws 0.1 mm. Mesofemur *ca.* 1.1 mm long; mesotibia *ca.* 0.9 mm, mesotarsus *ca.* 0.45 mm, mesotarsal claws stout, *ca.* 0.14 mm. Hind leg larger than others, metafemur stout and medially enlarged, maximal width *ca.* 0.36 mm, 1.2 mm long; metatibia 1.15 mm long, metatarsus long, *ca.* 0.5 mm long, metapretarsal claw 0.16 mm long. Tibial spines: protibia with f1, f2, f3, plus one more proximal (x); mesotibia with four spines m1, m2, m3, m4 plus one ventral spine (ma); metatibia with four spines h1, h2, h3, h4 (h1 and h4 small), plus two ventral spines (hb, hc) and a row of stout macrosetae. Eleven visible abdominal tergites, last one the smallest, lengths for TIV to apical terga measured dorsally (in mm): 0.31, 0.25, 0.31, 0.35, 0.22, 0.14, 0.11, 0.06. Total length of abdomen *ca.* 2.5 mm.

Styli not observed; cerci slender, short (0.2 mm), and with four cercomeres, basal cercomeres the widest and apical most the longest.

**Remarks:** Even if this fossil is partly damaged, we can undoubtedly assign it to the Mastotermitidae based on the five tarsomeres, head without fontanelle (even if partially destroyed, we did not notice any external groove or internal gland or structures suggesting the presence of a fontanelle), large pronotum as wide as head, slightly saddle-shaped, and cerci four-segmented. Additionally, *Milesitermes* gen. nov. differs from the only other Mastotermitidae soldier (*Anisotermes xiai*) from the Cretaceous period in having thin hooked mandibles without a basal tooth, pronotum trapezoidal-shaped, peculiar tibial spurs arrangement, and almost no pilosity (but possible problem of preservation) (Zhao *et al.*, 2019). In termites, workers/soldiers body length is about 0.8 times that of alates (Engel *et al.*, 2016) so that *Milesitermes* gen. nov. (body length 6.4 mm) does not belong to *Anisotermes xiai* (body length 12.9 mm).

*Milesitermes* gen. nov. differs from the soldiers of the extant *Mastotermes darwiniensis* and of the Miocene *Mastotermes electromexicanus* in its thinner mandible without a strong basal tooth and its pronotum trapezoidal.

An epicranial scar (plesiomorphy) could be present on the head of *Milesitermes* gen. nov. but the discovery of new specimens is necessary to confirm this hypothesis. Numerous wood fragments are embedded in the amber piece and may suggest a wood feeding habit. Note that Zhao *et al.* (2019) attributed a soldier to *Anisotermes xiai* (whose type is an alate specimen) on the basis of the unique presence of this species in the Burmese amber when they described it.

The peculiar shape of the mandible of *Milesitermes* gen. nov. is unknown because it has been damaged on this specimen. We consider unwise to derive any systematic affiliation based on the mere shape of this mandible. Nonetheless, note that soldiers of Hodotermitidae may have similar mandibles but they do not have five tarsomeres. Also, Hodotermitidae soldiers have their pronota narrower than their heads and do not possess additional spines on tibia. Furthermore, it is unlikely that *Milesitermes*

gen. nov. belong to the Hodotermitidae whose soldiers have heavily toothed mandibles, a feature we did not observe on *Milesitermes* gen. nov.

Family Rhinotermitidae Froggatt, 1897

Subfamily Heterotermitinae Froggatt, 1897

Genus *Reticulitermes* Holmgren, 1913

*Reticulitermes grimaldii* **sp. nov.** Jouault & Nel (Figs 3-4)

urn:lsid:zoobank.org:act:A25EC97F-73EA-4EF8-A30F-DF1B6F3F1516

**Holotype:** Number IGR.BA-020 (a nearly complete and well-preserved soldier).

**Etymology:** The specific epithet is a patronym honoring our colleague Pr. David A. Grimaldi, eminent American paleoentomologist, and specialist of Isoptera. The species epithet is to be treated as a noun in the genitive case.

**Locality and horizon:** In Baltic amber, Kaliningrad Oblast, Russia, Late Eocene (likely Priabonian, *ca.* 34–38 Ma).

**Diagnosis:** The new species can be readily distinguished from the two other *Reticulitermes* in Baltic amber, because it is the only soldier. Body and head medium of sized. Head capsule rectangular slightly tapering posteriorly, sides slightly convex. Labrum with four(?) apical setae. Mandibles elongated and strongly hooked in their apical third, right mandibles apparently slightly shorter than left one; left mandible overlapping right mandible. Fontanelle small situated close. Antennae moniliform with 14 antennomeres; antennal insertion surrounded by a small rim. Pronotum large, narrower than head, apparently slightly saddle-shaped with concave anterior margin; lateral margins nearly parallel, posterior margin slightly concave. Legs with tarsi tetramerous, tibial spur formula 3–2–2. Pro- and metatibia with a row of macrosetae. Abdomen plump; styli slender; cerci two-segmented.

**Description:** Soldier. Body length around *ca.* 5.25 mm from tip of mandible to apex of abdomen, but body is slightly twisted so total length slightly greater. Head massive, width *ca.* 1.05 mm, length *ca.* 2.25 mm from anterior margin of labrum to posterior margin of head, *ca.* 2.5 mm total (including mandibles); head capsule rectangular, tapering posteriorly, longer than wide; lateral margins subparallel to slightly convex; posterior border virtually separated from anterior margin of pronotum. Mandibles very heavily sclerotized, strongly prognathous; left mandible overlapping right mandible; mandible bases rather broad; right mandibles slightly shorter than left one but partly hidden; dentition not visible due to amber fractures, apparently absent, but, if present, only composed of minutes teeth at mandible bases; apex of left mandible slender, very pointed and hooked; left mandible 0.78 mm long, greatest exposed width *ca.* 0.15 mm. Maxillary palps with at least four palpomeres, basal palpomere shortest, ultimate one apparently the longest; labial palps not visible. Galea, cardo, stipes, and other mouthparts not visible (covered by a white veil). Cervical sclerites not visible. Labrum long, triangular with convex sides, 0.45 mm wide x 0.35 mm long, covered with sparse short appressed setae, apically with four(?) distinct long setae on margin. Anteclypeus shallow with anterior margin convex and posterior margin slightly concave, 0.44 mm wide, 0.08 mm long; postclypeus somewhat rectangular, 0.55 mm wide, 0.11 mm long. Clypeus without any projection; postclypeus flat. Fontanelle preserved as a small concavity situated posterior to clypeus; setulae surrounding fontanelle present. Compound eye spot not discernable, absent or inconspicuous. Antenna with 14 preserved antennomeres, antenna insertion delimited by a small rim. Pronotum large, narrower than head, partially bend due to preservation, apparently slightly saddle-shaped (maybe due to preservation), with concave anterior margin, median portion raised longitudinally, lateral parts depressed; lateral margins nearly parallel (very slightly convex), posterior margin slightly concave; pronotal dimensions: medial length 0.35 mm; greatest length 0.48 mm; greatest width 0.75 mm. Meso- and metanotum slightly convex in lateral view but not describable. Legs with tarsi tetramerous, tibiae spinose, tibial spines slightly symmetrical and smooth; arolium absent between pretarsal claws. Foreleg smallest, procoxa small, protibia slender, *ca.* 0.46 mm long, protarsus 0.22 mm long, pretarsal

claws slightly smaller than metapretarsal claws; profemur thick, stout. Mid legs partly destroyed during preparation. Hindleg apparently the largest, metacoxa 0.3 mm long (L), 0.2 mm wide (W); metatrochanter 0.16 mm L, 0.08 mm W; metafemur: 0.75 mm L, 0.23 mm W; metatibia swollen apically 0.83 mm L, 0.11 W, with two spines, metatarsus long, 0.33 mm L, metapretarsal claw *ca.* 0.07 mm L. Tibial spines: protibia with three spines f1, f2, f3, without a row of stout ventral setae; mesotibiae with two spines m1, m2; metatibia with two spines: h2, h3 and a row of stout ventral setae. At least eight abdominal sternites visible ventro-laterally, lengths along midline, from SII–SVIII (in mm): 0.22, 0.18, 0.18, 0.18, 0.07, 0.15, 0.11. Total length of abdomen *ca.* 1.75 mm. Styli *ca.* 0.07 mm long; cerci slender, short (*ca.* 0.12 mm), and two-segmented.

Color. Head clearly orange, except black mandibles and brown labrum; rest of body grayish white.

**Remarks:** Based on the presence of four tarsomeres, head with fontanelle (hole partially visible), flat pronotum, mandible without serrations along the inner margins (maybe some at the base, but not visible), we can undoubtedly assign *Reticulitermes grimaldii* sp. nov. to the Rhinotermitidae. Within this family, *Reticulitermes grimaldii* sp. nov. keys out in the Heterotermitinae because of the eye spot absent or inconspicuous, the head with a small fontanelle, the absence of a groove from the fontanelle to the base of the clypeus, and the head with subparallel sides (Emerson, 1971). The presence of setulae surrounding the fontanelle is also distinctive of the Heterotermitinae (Engel *et al.*, 2009).

The Heterotermitinae comprise the genera *Heterotermes* Froggatt, 1897 and *Reticulitermes*. Despite the fact that the mandibles cross, the flat postclypeus exclude any affinity with *Heterotermes* (Scheffrahn & Su, 1995: Table 1). We assigned specimen IGR.BA-020 to the genus *Reticulitermes* based on its flat postclypeus, its mandibles distinctly hooked at tip, and its tongue-shaped labrum (Krishna *et al.*, 2013). Carrijo *et al.* (2020) proposed a phylogeny of the New World *Heterotermes* and have highlighted the hyaline labrum of soldiers as a generic character (Carrijo *et al.*, 2020: figs 1B,C), while the labrum in the genus *Reticulitermes* is fully sclerotized. This strengthens our taxonomic attribution. Interestingly, fossils of the genus *Reticulitermes* are rather frequent in the Baltic amber (Nel & Paicheler, 1993), with two species described from alate specimens, viz. *R.*

*antiquus* (Germar, 1813) and *R. minimus* Snyder, 1928, making comparisons with the newly described soldier specimen impossible. Engel *et al.* (2007a) indicated that *R. antiquus* is the most common termite in Baltic amber. Additionally, these authors have proposed to distinguished *R. antiquus* from *R. minimus* by its larger body size (length of forewing from basal suture 6.5–8.8 mm in *R. antiquus* vs. 3.94 mm in *R. minimus*) and more numerous antennomeres (17–20 in *R. antiquus* vs. 13–14 in *R. minimus*) (Engel *et al.*, 2007a). The size of *Reticulitermes grimaldii* sp. nov. could match with *R. antiquus* since termites soldiers are rarely larger than alates. However, the number of antennal segments cannot be used to assign *Reticulitermes grimaldii* sp. nov. to one of the previously described species since it varies between soldier and alate castes. In termites, a general trend established that the body length of workers and soldiers relative to alates is close to 0.8 (Engel *et al.*, 2016 page 6 and fig. S3). Therefore, *Reticulitermes grimaldii* sp. nov. cannot be attributed to *R. minimus* because its body is nearly twice as long. Similarly, *Reticulitermes grimaldii* sp. nov. cannot be attributed to *R. antiquus* since the soldier is slightly longer than the alates of *R. antiquus*.

### *Phylogenetic analyses*

*Milesitermes engeli* gen. et sp. nov. and *Reticulitermes grimaldii* sp. nov. are nested, respectively, within Mastotermitidae and Rhinotermitidae in BI and MP (Figs 5-6; Supp. fig. 1), confirming our taxonomic attributions. The ‘mid’-Cretaceous genus *Krishnatermes* Engel *et al.*, 2016 is closely related to the Mastotermitidae as the sister taxon of the Middle Eocene *Idanotermes desioculus* Engel, 2008. In terms of topologies, all BI analyses resulted in very similar tree reconstructions, except for the poorly supported (PP < 0.5) relationships within the ‘*Meiatermes*-grade’.

In addition to defining the relationships of the two new fossil taxa, our main aim was to refine time divergence estimates in Isoptera (Fig. 5, Script\_FBD-1part). All tip-dating analyses (run with the FBD model, except one analysis with a uniform strict clock) push back the time divergence estimates of stem- and crown-Isoptera of several tens of Myrs: 232 Ma (172–362 Ma min and max values of 95% HPD) and 205 Ma (171–234 Ma) for stem- and crown Isoptera across all FBD

analyses, respectively, vs 189 Ma (147–252 Ma) and 144 Ma (137–167 Ma 95% HPD) in the node-dating analyses (Fig. 6A, Script\_node-dating). In the tip-dating analysis with one partition (Fig. 5), the most recent common ancestor (MRCA) of Euisoptera is estimated to have arisen 185 Ma (161–206 Ma 95% HPD). The MRCA of Neoisoptera is estimated to have arisen 109 Ma (99–126 Ma 95% HPD), while the MRCA of Termopsidae is estimated to have arisen 54 Ma (37–83 Ma 95% HPD). Archotermopsidae and Hodotermitidae are sister-taxa and their crown-groups would date back from the K/T and the Oligocene/Miocene boundaries, respectively (68 Ma, 42–101 95% HPD and 28 Ma, 6–56 95% HPD). Extant Stolotermitidae have their MRCA from the Eocene (38 Ma, 9–75 95% HPD), while their oldest relatives (from the genus *Cosmotermes*) would date back to the Lower Cretaceous (115 Ma, 101–137 95% HPD). As for Kalotermitidae, the crown-group would have originated during the Paleocene (58 Ma, 36–86 95% HPD), while the stem-Kalotermitidae would date back to the Lower Cretaceous (126 Ma, 110–146 95% HPD).

Overall, the oldest age estimates are found, for all nodes, when a uniform clock is used. The tip-dating analysis that gives the youngest age (viz. with fixed calibrations and a diversity sampling), still produces older mean estimates than node-dating analyses, except for the shallowest nodes. Time divergence estimates for the main isopteran lineages are summarized across all analyses in Table 1, whereas several priors, statistics and parameter values are summarized in Supporting Information.

Partitioning the data reveals that each partition (alates/workers, soldiers, and life-history traits) has its own history, as shown with their relative rates of changes. While higher rates were found along the branch leading to termites without any partitioning (Figure 6), higher rates were found either in most of the deepest nodes (alates/workers partition), for Nasutitermitinae (soldiers partition), or for the outgroups (life-history traits partition).

## Discussion

### *A possible Triassic/Jurassic origin of eusociality*

If we assume that tip-dating results better reflect the timing of evolution of termites than node-dating analyses (see below), crown-Isoptera would have arisen around the Late Triassic / Early Jurassic boundary (ca. 205 Ma, 182–233 mean 95% HPD), 50–60 Ma earlier than currently thought (as reflected with node-dating results: 144 Ma, 137–166 mean 95% HPD). This suggests an even older origin of stem-Isoptera, dating back to the Late Triassic. Those age estimates were consistently found across all tip-dating analyses, even with very flat priors or when priors were centered on much younger ages (e.g. mean age for crown Isoptera set to 144 Ma); some tip-dating analyses even produced older age estimates but those might be biased (e.g. random sampling, see below).

The disagreements between node- and tip-dating estimates underline that further investigations are needed to clarify the timing of termite diversification and of the origin of their eusociality. Several reasons may explain those differences (Matzke & Wright, 2016), including recent fossil discoveries that could not be included in earlier studies (Bourguignon *et al.*, 2015, 2018; Legendre *et al.*, 2015; Engel *et al.*, 2016; Bucek *et al.*, 2019; Evangelista *et al.*, 2019; Zhao *et al.*, 2019, 2020a; but see Ware *et al.*, 2010 for older estimates). In many taxonomic groups, recent fossil discoveries have impacted our understanding of their timing of evolution. Termites are not an exception (e.g. Selden *et al.*, 2011; Huang *et al.*, 2012, 2013; Toussaint & Condamine, 2016; Nicholson *et al.*, 2015).

Our dating increases the discrepancy between phylogenetic age estimates and the termite fossil record. Such a mismatch is not uncommon and is often explained by fossilization biases. Even at uncontroversial times—i.e. when termites were undoubtedly present—their presence in the fossil record might be scarce. Less than 1% of all insect specimens from the Early Cretaceous are termites (Engel *et al.*, 2009: Table 2) and there is currently no Triassic or Jurassic record of termites. Putative termite nests have been suggested from the Triassic and Early Jurassic (Hasiotis and Dubiel, 1995; Bordy *et al.*, 2004) but those ichnofossils remain controversial (Genise, 2016). Our datings of crown-Isoptera, concomitant to those putative nests, could fuel the debate around those nests and their significance for the origin of eusociality, although the construction of large mounds is a derived trait,

acquired more recently, within termites. Irrespectively of those dubious fossils (Legendre et al. 2015), nest structures in termites result from advanced cooperation among colony members, revealing highly integrated social systems (Grassé, 1986; Invernizzi & Ruxton, 2019). The capacity to build a nest was probably inherited by the common ancestor of the crown-Isoptera (Mizumoto and Bourguignon, 2020). Although nest building does not require a soldier caste, it does require a worker caste ('true' workers or pseudergates), which has been found in Early Cretaceous deposits for the latest (Martínez-Delclòs & Martinell, 1995). Recent descriptions of workers and soldiers (Engel *et al.*, 2016; Zhao *et al.*, 2019, 2020a) have confirmed that eusociality was already established in the Early to 'mid'-Cretaceous.

The oldest termite fossils correspond to alates, which are indecisive for deciphering the origin of eusociality. Those fossils have wing sutures, like living alate termites, suggesting that these ancient termites had adult swarms and lived the rest of their life in hidden, cryptic environments. But it does not mean that they were eusocial insects. In other words, although it is reasonable to think that fossil taxa of crown-Isoptera were eusocial, alates from stem-Isoptera do not inform about the putative eusociality of those stem-lineages.

Living in cryptic environments during the Late Triassic-Early Jurassic was undoubtedly advantageous because dinosaurs, small lizards, and mammals diversified at that time, with at least some of those mammals that were insectivorous (Luo, 2007; Melo *et al.*, 2019). The Late Jurassic mammal *Fruitafossor* convergently developed the main morphological characters that allow extant armadillos and aardvarks to dig the ground and feed on termite nests (Luo & Wible, 2005; Luo, 2007). Interestingly, *Fruitafossor* was found in the Late Jurassic Morrison Formation (Colorado, USA), in layers where some putative termite nests were also described (Engelmann, 1999; Koch *et al.*, 2006, Smith et al., 2020). Its presence may provide additional support to the hypothesis that termite nests and eusociality were already established at that time, sufficient to provide a food source for a highly specialized mammal. But, alternatively, *Fruitafossor* might also have fed on other unknown insects, even if there is no obvious candidate group in the rather well-known Late Jurassic entomofauna; those

hypotheses need to be investigated further. As indicated by the fossil record and the estimates of isopteran stem and crown ages, it is highly probable that the cryptic termites became eusocial during the period between the Early and Late Jurassic.

It is however unclear whether first termites (i.e. stem-Isoptera but also †*Cratomastotermes*, †*Baissatermes*, etc.) were deprived of a soldier caste like the first diverging lineages of corbiculates, some halictine bees, and ants (†Haidomyrmecinae, †Sphecomyrminae, and poneromorphs). Similarly, it is unclear whether stem-lineages of termites had a worker caste. But if they did, it is often believed that the polymorphism between workers and reproducers was reduced (Engel *et al.*, 2007b; Michener, 1974; Hölldobler & Wilson, 1990; Barden & Grimaldi, 2016).

#### *Refining stem and crown-ages within Isoptera and identifying ghost lineages*

Differentiating stem- from crown-groups is pivotal to our understanding of how lineages waxed and waned (Budd & Mann 2020). In Isoptera, the difference has sometimes been elusive for three reasons. First, the termite fossil record is full of gaps, for instance between the ‘mid’-Cretaceous and the Paleocene-Middle Eocene. Second, some families (e.g. Mastotermitidae) are only represented by one or two species. Third, the assignment of certain fossil species to extant lineages is questionable due to their poor preservation. All these issues obfuscate the delineation between stem- and crown-groups, and lead to misestimating their ages. It might, however, be clarified with tip-dating analyses wherein fossils are included in the phylogenetic reconstructions.

With *Mastotermes darwiniensis* as its single living species and several extinct species sharing plesiomorphies, the Mastotermitidae is one of the families for which delineating stem- and crown-groups is the most complicated (Zhao *et al.*, 2019). Although its phylogenetic position as the first-diverging lineage within Isoptera is well-established (e.g. Kambhampati *et al.*, 1996; Donovan *et al.*, 2000; Thompson *et al.*, 2000; Inward *et al.*, 2007; Legendre *et al.*, 2008), its synapomorphy that could be discernable on fossils has been clarified only recently: a thick and sclerotized M vein, stronger than CuA (Zhao *et al.*, 2019). On the basis of this synapomorphy, the family includes now six genera,

i.e., *Anisotermes*, *Blattotermes*, *Garmitermes*, *Mastotermes*, *Milesitermes* gen. nov., and *Miotermes*. Zhao *et al.* (2019: 621) excluded the genera *Valditermes*, *Idanotermes*, and *Khanitermes* from the Mastotermitidae. The relationships of *Spargotermes* remain uncertain (Wappler & Engel, 2006; Bezerra *et al.*, 2020). The genus *Mastotermes* is possibly not monophyletic but its definition is out of the scope of this paper. We dated this highly-supported clade from the Early Cretaceous (130 Ma, 108–161 95% HPD). Stem-Mastotermitidae—containing by definition all extinct organisms more closely related to crown-Mastotermitidae than to any other crown-group (Budd and Mann, 2020)—would include *Idanotermes*, *Krishnatermes*, *Valditermes*, *Cratomastotermes*, *Carinatermes*, *Mylacrotermes* and some *Meiatermes* species, and may have originated in the Early Jurassic (188 Ma, 166–209 95% HPD). The composition of stem-Mastotermitidae is, however, not clearly settled because deeper nodes in the phylogeny of termites are weakly supported. This is notably due to the quality of the fossil record, with several species of the so-called *Meiatermes*-grade based on incomplete specimens.

Similarly, we have clarified the delineation between stem- and crown-groups of the following families: Archotermopsidae, Stolotermitidae, Hodotermitidae, and Kalotermitidae. Our age estimates agree with those previously found for the Archotermopsidae but not for the Hodotermitidae (Bourguignon *et al.*, 2015; Bucek *et al.*, 2019). The split between those two families would have occurred in the Early Cretaceous (116 Ma, 73–160 mean 95% HPD), revealing a ghost lineage of ca. 90 Ma for Hodotermitidae. However, in all recent molecular works (e.g. Bourguignon *et al.*, 2015, 2018; Legendre *et al.*, 2015), Hodotermitidae are nested within Archotermopsidae, contrary to what we found here. This disagreement, which might be reduced with future works on Hodotermitid fossils (CJ in prep.), unavoidably affects dating estimates. Another ghost lineage, the one leading to Stolotermitidae, has been recently investigated (Zhao *et al.*, 2020a). This study and ours rely on the same dataset and their results concur; we nonetheless suggest a putative stem-Stolotermitidae (i.e. *Tanytermes*) that would require further investigation as its phylogenetic position is poorly supported.

Ghost lineages have always challenged the understanding of organism diversification. They emphasize how rocks and clocks disagree, how the fossil record and phylogenetic dating estimates might diverge (Ronquist *et al.*, 2016). Gaps in the insect fossil record are notorious (Nel *et al.*, 2018) and are more prone to occur for some lineages than others. For termites, the putative cryptic way of life of stem-lineages was an unfavorable condition for their fossilization, which might explain the absence of a fossil record in the Early and Middle Jurassic. But even some lineages with important mating swarms, like the Hodotermitidae, might show important gaps in their fossil record. Underlining those gaps and refining their temporal delimitation contribute to clarify which deposits should be further investigated, and hopefully make termite rocks and clocks converge.

#### *Better models for better dating estimates*

Because of the well-identified limitations of node-dating analyses, tip-dating analyses are becoming popular (Parham *et al.*, 2012; Ronquist *et al.*, 2012; Heath *et al.*, 2014; Matzke & Wright, 2016; Simões *et al.*, 2020). They are, however, not devoid of their own limitations, which has occasionally triggered some doubts in their resulting age estimates, which might have seemed unreasonably old (e.g. Arcila & Tyler, 2017). Several reasons have been suggested from the lack of a FBD process, to inaccurate topologies and inadequate models of evolution (Arcila & Tyler, 2017; Luo *et al.*, 2020; Simões *et al.*, 2020). Here, tip-dating analyses all provide older estimates than node-dating analyses. However, to both test and circumvent the aforementioned potential issues, we have implemented several FBD-based analyses and constrained a few nodes in the topology. Using uniform or fixed calibrations for fossil tips resulted in similar datings (Supplementary Information). Fixed calibrations slightly pulled down time divergence estimates, but using uniform priors seems more appealing and relevant because the exact age of each fossil is unknown. Likewise, we have tested different priors (i.e. clockrate and speciation priors, mean age for the ingroup) but it did not significantly change our results. One parameter—allowing fossil ancestor to be sampled or not—had a deeper impact on dating estimates but none of the analyses resulted in ages as young as in the node-

dating analyses. Analyses wherein fossil ancestor were allowed to be sampled even produced the oldest estimates (if we omit the analysis with a uniform clock), but some parameter estimates are dubious (e.g. estimated mean of branch rate variance) so that ages estimated from those analyses should be interpreted with caution. A recent study on sphenodontian reptiles came to the same conclusion regarding the negative impact of sampling for ancestors in dating estimates relying only on morphological datasets (Simões *et al.*, 2020).

Overall, we consider the dating estimates produced with the birth-death-serial-sampling (BDSS) models as reasonable up-to-date hypotheses, while the estimates resulting from sampled-ancestor BDSS are dubious. Note that for some of the shallowest nodes, the topology—and thus the associated datings—is inaccurate, which is a typical consequence of a reduced morphological dataset (Luo *et al.*, 2020). It has arguably a very limited effect on dating estimates of the deepest nodes, those we mostly focused on in this work, especially knowing that we include numerous fossil taxa in our analyses (Luo *et al.*, 2020).

Beyond including more fossil taxa into tip-dating or total-evidence phylogenetic analyses to produce more robust age estimates, improving the models for morphological data is a complementary direction (Wright & Hillis, 2014; Simões *et al.*, 2020). Herein, we have tested a Mkv and Mkv + G models, as well as the impact of morphological data partitioning. It had an insignificant effect on dating estimates but it unsurprisingly revealed that each partition had its own evolutionary trajectory. In other words, evolutionary rates for soldier-related characters differ from the rates of worker/alate-related characters. The differences are striking for some lineages (e.g. within Termitidae; Figure 6) and a partitioning approach should be more often used for morphological data, like it is now routinely done with molecular data. Partitioning morphological data might affect tree reconstructions and dating estimates, or be the foundation for studies aiming at deciphering morphological evolution (e.g. Zhang and Wang, 2019). Whatever the aim, the ongoing developments in models for morphological data must go on (e.g. O'Reilly *et al.*, 2016; Puttick *et al.*, 2017; Goloboff *et al.*, 2018).

## Conclusion

Time divergence estimates of the Isoptera and of some constitutive families may be older than previously stated. If our results are correct, the crown Isoptera may have arisen ca. 205 Ma (171–234 Ma), contrasting with most molecular-based node-dating analyses (between 134–165 Ma) (Bourguignon *et al.*, 2015; Legendre *et al.*, 2015; Evangelista *et al.*, 2019; Bucek *et al.*, 2019). We infer those results from the termite fossil record that we have enriched with two new species from the Burmese mid-Cretaceous amber and Baltic Eocene amber. This suggests that termites have developed a ‘highly specialized’ eusociality with a tripartite caste system before ants and other eusocial taxa. This social organization might have influenced their ability to survive mass extinctions (e.g. Bakker, 1998) or favored the appearance of other modern eusocial insects such as Hymenoptera (particularly wasps and ants) by providing an abundant food source. Additionally, acquiring a eusocial system has certainly enabled termites to become a group with a major ecological role in various palaeoenvironments. By refining and providing new time divergence estimates of the crown-groups of termite families, our study might allow better palaeoecological inferences from their extant representatives. Clarifying the distinction between stem- and crown-groups among termite families will also contribute to a better understanding of termite diversification.

Although we have proposed a new hypothesis for the tempo of diversification of termites, further analyses and material are needed, especially for the ‘*Meiatermes*-grade’, whose lineages probably belong to the stem-Mastotermitidae or to a transition stage between Mastotermitidae and Euisoptera. Further advances might also be achieved from improvements in evolutionary models for morphological data like our partitioned analyses suggest.

## Data availability statement

The data that support the findings of this study are available from the corresponding authors upon reasonable request.

### **Author contributions**

C.J. and F.L. are first authors with equal rank and performed the phylogenetic analyses; C.J. and A.N. coordinated the manuscript, wrote the descriptions, and prepared the figures; all authors drafted the manuscript.

### **Acknowledgments**

CJ is grateful to Dr. Phillip Barden (NJIT, Newark; AMNH, New York, USA) who provided literature on phylogenetic analyses. We thank three anonymous reviewers for their constructive comments.

### **Conflicts of interest statement**

The authors declare that there are no conflicts of interest.

### **Supplementary files:**

**Appendix 1.** Morphological matrix with MrBayes scripts.

**Appendix 2.** List of character states.

**Appendix 3.** Justifications of calibrations implemented in dating analyses.

**Appendix 4.** Results of statistics and parameter values recorded for each model and prior.

**Supplementary fig. 1.** Strict consensus cladogram generated from parsimony analysis. Tree length 354 steps, consistency index (CI) 0.41, homoplasy index (HI) 0.58, retention index (RI) 0.84. Values in black above branches represent bootstrap percentages > 50% (majority-rule consensus) while red values represent Bremer indices.

### **References**

Aleksandrova, G.N. & Zaporozhets, N.I. (2008) Palynological characteristics of Upper Cretaceous and Paleogene deposits on the west of the Sambian Peninsula (Kaliningrad region), Part 2.

*Stratigraphy and Geological Correlation*, **16**, 528–539.

<http://dx.doi.org/10.1134/S0869593808050067>.

Alekseev, V.I. (2018) The revision of gymnosperm species from Eocene Baltic amber. *Botanicheskii Zhurnal*, **103**, 229–245.

Arcila, D., & Tyler, J. C. (2017) Mass extinction in tetraodontiform fishes linked to the Palaeocene–Eocene thermal maximum. *Proceedings of the Royal Society B: Biological Sciences*, **284**(1866), 20171771. <https://doi.org/10.1098/rspb.2017.1771>.

Bakker, R.T. 1998. Dinosaur mid-life crisis: the Jurassic-Cretaceous transition in Wyoming and Colorado. *New Mexico Museum of Natural History and Science Bulletin*, **14**, 67–78.

Barido-Sottani, J., Aguirre-Fernández, G., Hopkins, M.J., Stadler, T. & Warnock, R. (2019) Ignoring stratigraphic age uncertainty leads to erroneous estimates of species divergence times under the fossilized birth–death process. *Proceedings of the Royal Society B*, **286**, 20190685. <https://doi.org/10.1098/rspb.2019.0685>.

Barden P. & Engel M.S. (2020) Fossil social insects. In: Starr C. (eds) *Encyclopedia of Social Insects*. Springer, Cham. [https://doi.org/10.1007/978-3-319-90306-4\\_45-1](https://doi.org/10.1007/978-3-319-90306-4_45-1).

Barden, P. & Grimaldi, D.A. (2016) Adaptive radiation in socially advanced stem-group ants from the Cretaceous. *Current Biology*, **26**, 515–521. <https://doi.org/10.1016/j.cub.2015.12.060>.

Bezerra, F.I., Mendes, M. & De Souza, O. (2020) New record of Mastotermitidae from Fonseca Basin, Eocene-Oligocene boundary of southeastern Brazil. *Biologia*, **75**, 1881–1890. <https://doi.org/10.2478/s11756-020-00441-x>.

Bordy, E.M., Bumby, A.J., Catuneanu, O. & Eriksson, P.G. (2004) Advanced Early Jurassic termite (Insecta: Isoptera) nests: evidence from the Clarens Formation in the Tuli Basin, Southern Africa. *Palaios*, **19**, 68–78. [https://doi.org/10.1669/0883-1351\(2004\)019%3C0068:AEJTII%3E2.0.CO;2](https://doi.org/10.1669/0883-1351(2004)019%3C0068:AEJTII%3E2.0.CO;2).

Bordy, E.M., Bumby, A.J., Catuneanu, O. & Eriksson, P.G. (2009) Possible trace fossils of putative termite origin in the Lower Jurassic (Karoo Supergroup) of South Africa and Lesotho. *South African Journal of Science*, **105**, 356–362.

[http://www.scielo.org.za/scielo.php?script=sci\\_arttext&pid=S0038-23532009000500012&lng=en&nrm=iso](http://www.scielo.org.za/scielo.php?script=sci_arttext&pid=S0038-23532009000500012&lng=en&nrm=iso).

- Bordy, E.M., Knoll, F. & Bumby, A. (2010) New data on the palaeontology and sedimentology of the Lower Jurassic Lisbon Formation (Karoo Supergroup), Ellisras Basin, South Africa. *Neues Jahrbuch für Geologie und Paläontologie, Abhandlungen*, **258**, 145–155. <https://doi.org/10.1127/0077-7749/2010/0091>.
- Bourguignon, T., Lo, N., Cameron, S.L., Šobotník, J., Hayashi, Y., Shigenobu, S., Watanabe, D., Roisin, Y., Miura, T. & Evans, T.A. 2015. The evolutionary history of termites as inferred from 66 mitochondrial genomes. *Molecular Biology and Evolution*, **32**, 406–421. <https://doi.org/10.1093/molbev/msu308>.
- Bourguignon, T., Tang, T., Ho, S.Y.W., Juna, F., Wang, Z., Arab, D.A., Cameron, S.L., Walker, J., Rentz, D., Evans, T.A. & Lo, N. (2018) Transoceanic dispersal and plate tectonics shaped global cockroach distributions: evidence from mitochondrial phylogenomics. *Molecular Biology and Evolution*, **35**, 970–983. <https://doi.org/10.1093/molbev/msy013>.
- Bremer, K. (1994) Branch support and tree stability. *Cladistics*, **10**, 295–304. <https://doi.org/10.1111/j.1096-0031.1994.tb00179.x>.
- Brullé, G.A. (1832) Expédition scientifique de Morée. Section des sciences physiques zoologie. Deuxième section - des animaux articulés [Vol. 3, part 1]. Paris, F.G. Levrault, 400 pp.
- Bucek, A., Šobotník, J., He, S., Shi, M., McMahon, D.P., Holmes, E.C., Roisin, Y., Lo, N. & Bourguignon, T. (2019) Evolution of termite symbiosis informed by transcriptome-based phylogenies. *Current Biology*, **29**, 3728–3734. <https://doi.org/10.1016/j.cub.2019.08.076>.
- Budd, G.E. & Mann, R.P. (2020) The dynamics of stem and crown groups. *Science Advances*, **6**, eaaz1626. <https://doi.org/10.1126/sciadv.aaz1626>.
- Carrijo, T.F., Pontes-Nogueira, M., Santos, R.G., Morales, A.C., Canello, E.M. & Scheffrahn, R.H. (2020) New World *Heterotermes* (Isoptera, Rhinotermitidae): molecular phylogeny, biogeography

- and description of a new species. *Systematic Entomology*, **45**, 527–539.  
<https://doi.org/10.1111/syen.12412>.
- Cockerell, T.D.A. (1916) Insects in Burmese amber. *American Journal of Science* (4), **42**, 135–138.  
<https://doi.org/10.2475/ajs.s4-42.248.135>.
- Condamine, F.L., Nel, A., Grandcolas, P. & Legendre, F. (2020) Fossil and phylogenetic analyses reveal recurrent periods of diversification and extinction in dictyopteran insects. *Cladistics*, **36**, 394–412. <https://doi.org/10.1111/cla.12412>.
- Cruickshank, R.D. & Ko, K. (2003) Geology of an amber locality in the Hukawng Valley, northern Myanmar. *Journal of Asian Earth Sciences*, **21**, 441–455. [https://doi.org/10.1016/S1367-9120\(02\)00044-5](https://doi.org/10.1016/S1367-9120(02)00044-5).
- Desneux, J. (1904) A propos de la phylogénie des Termitidae. *Annales de la Société Entomologique de Belgique*, **48**, 278–286.
- Dillard, J. & Benbow, M.E. (2020) From symbionts to societies: how wood resources have shaped insect sociality. *Frontiers in Ecology and Evolution*, **8**, 1–8.  
<https://doi.org/10.3389/fevo.2020.00173>.
- Djernæs, M., Klass, K.-D. & Eggleton, P. (2015) Identifying possible sister groups of Cryptocercidae+Isoptera: A combined molecular and morphological phylogeny of Dictyoptera. *Molecular Phylogenetics and Evolution*, **84**, 284–303.  
<https://doi.org/10.1016/j.ympev.2014.08.019>.
- Donovan, S.E., Jones, D.T., Sands, W.A. & Eggleton, P. (2000) Morphological phylogenetics of termites (Isoptera). *Biological Journal of the Linnean Society*, **70**, 467–513.  
<https://doi.org/10.1111/j.1095-8312.2000.tb01235.x>.
- dos Reis, M., Donoghue, P.C.J. & Yang, Z. (2016) Bayesian molecular clock dating of species divergences in the genomics era. *Nature Reviews Genetics*, **17**, 71–80.  
<https://doi.org/10.1038/nrg.2015.8>.

- Emerson, A.E. (1971) Tertiary fossil species of the Rhinotermitidae (Isoptera), phylogeny of genera, and reciprocal phylogeny of associated Flagellata (Protozoa) and the Staphylinidae (Coleoptera). *Bulletin of the American Museum of Natural History*, **146**, 243–303. <http://hdl.handle.net/2246/1093>.
- Engel, M.S. (2019) Termite evolution: a primal knock on wood or a hearty mouthful of dirt. *Current Biology*, **29**, PR1126–R1129. <https://doi.org/10.1016/j.cub.2019.09.016>.
- Engel, M.S., Grimaldi, D. & Krishna, K. (2007a) Synopsis of Baltic amber termites (Isoptera). *Stuttgarter Beiträge zur Naturkunde (B)*, **372**, 1–20.
- Engel, M.S., Grimaldi, D.A. and Krishna, K. (2007b) Primitive termites from the Early Cretaceous of Asia (Isoptera). *Stuttgarter Beiträge zur Naturkunde (B)*, **371**, 1–32.
- Engel, M.S., Grimaldi, D.A. & Krishna, K. (2009) Termites (Isoptera): their phylogeny, classification, and rise to ecological dominance. *American Museum Novitates*, **3650**, 1–27. <http://hdl.handle.net/2246/5969>.
- Engel, M.S., Barden, P., Riccio, M.L. & Grimaldi, D.A. (2016) Morphologically specialized termite castes and advanced sociality in the Early Cretaceous. *Current Biology*, **26**, 522–530. <http://dx.doi.org/10.1016/j.cub.2015.12.061>.
- Engelmann, G.F. (1999) Stratigraphic and geographic distribution of fossils in the upper part of the Upper Jurassic Morrison Formation of the Rocky Mountain region. pp. 115–120. In: Gillette, D.D. (ed.). Vertebrate paleontology in Utah. Vertebrate fossils of Utah. Miscellaneous Publication, Utah Geological Survey, Salt Lake City, 99 (1), i–xiv, 1–553.
- Evangelista, D.A., Wipfler, B., Béthoux, O., Donath, A., Fujita, M., Kohli, M.K., Legendre, F., Liu, S., Machida, R., Misof, B., Peters, R.S., Podsiadlowski, L., Rust, J., Schuette, K., Tollenaar, W., Ware, J.L., Wappler, T., Zhou, X., Meusemann, K. & Simon, S. (2019) An integrative phylogenomic approach illuminates the evolutionary history of cockroaches and termites (Blattodea). *Proceedings of the Royal Society (B) Biological Sciences*, **286**, 20182076. <http://dx.doi.org/10.1098/rspb.2018.2076>.

- Felsenstein, J. (1985) Confidence limits on phylogenies: an approach using the bootstrap. *Evolution*, **39**, 783–391. <https://doi.org/10.1111/j.1558-5646.1985.tb00420.x>.
- Froggatt, W.W. (1897) Australian Termitidae. Part 2. *Proceedings of the Linnean Society of New South Wales*, **21**, 510–552.
- Gavryushkina A., Welch D., Stadler T. & Drummond A.J. (2014) Bayesian inference of sampled ancestor trees for epidemiology and fossil calibration. *PLoS Computational Biology*, **10**, e1003919. <https://doi.org/10.1371/journal.pcbi.1003919>.
- Genise, J.F. (2016) Ichnoentomology: insect traces in soils and paleosols. *Topics in Geobiology*, **37**, i-xxviii + 1–695. <https://doi.org/10.1007/978-3-319-28210-7>.
- Genise, J.F., Bellosi, E.S., Melchor, R.N. & Cosarinsky, M.I. (2005) Comment — advanced Early Jurassic Termite (Insecta: Isoptera) nests: evidence from the Clarens Formation in the Tuli Basin, Southern Africa. *Palaios*, **20**, 303–308. <https://doi.org/10.2110/palo.2004.p05-C01>.
- Germar, E.F. (1813) Insecten in Bernstein eingeschlossen, beschrieben aus dem academischen Mineralien-Cabinet zu Halle. *Magazin der Entomologie*, **1**, 11–18.
- Goloboff, P.A., Torres, A. & Arias, J.S. (2018) Weighted parsimony outperforms other methods of phylogenetic inference under models appropriate for morphology. *Cladistics*, **34**, 407–437. <https://doi.org/10.1111/cla.12205>.
- Grandcolas, P., D'Haese, C. (2002) The origin of a ‘true’ worker caste in termites: phylogenetic evidence is not decisive. *Journal of Evolutionary Biology*, **15**, 885–888. <https://doi.org/10.1046/j.1420-9101.2002.00451.x>.
- Grassé, P.P. (1986) Comportement – socialité – écologie – évolution – systématique. *Termitologia. Anatomie – physiologie – biologie – systématique des termites*. Fondation Singer-Polignac, Masson (publ.), Paris, **3**, 1–715.
- Grimaldi, D.A., Engel, M.S. & Nascimbene, P.C. (2002) Fossiliferous Cretaceous amber from Myanmar (Burma): its rediscovery, biotic diversity, and paleontological significance. *American Museum Novitates*, **3361**, 1–72. <http://hdl.handle.net/2246/2914>.

- Grimaldi, D. & Engel, M.S. (2005) *Evolution of the insects* (Cambridge: Cambridge University Press).
- Grimaldi, D. & Ross, A. (2017) Extraordinary lagerstätten in amber, with particular reference to the Cretaceous of Burma. In: Fraser, N.C. & Sues, H.-D. (eds.), *Terrestrial conservation lagerstätten: Windows into the evolution of life on land*. Dunedin Academic Press, Edinburgh, pp. 287–342.
- Hasiotis, S.T. & Dubiel, R.F. (1995) Termite (Insecta: Isoptera) nest ichnofossils from the upper triassic chinle formation, petrified forest national park, Arizona. *Ichnos*, **4**, 119–130. <https://doi.org/10.1080/10420949509380119>.
- Heath, T.A., Huelsenbeck, J.P. & Stadler, T. (2014) The fossilized birth-death process for coherent calibration of divergence-time estimates. *Proceedings of the National Academy of Sciences of the USA*, **111**, E2957–E2966. <https://doi.org/10.1073/pnas.1319091111>.
- Hillis, D.M. & Bull, J.J. (1993) An empirical test of bootstrapping as a method for assessing confidence in phylogenetic analysis. *Systematic Biology*, **42**, 182–192. <https://doi.org/10.1093/sysbio/42.2.182>.
- Hölldobler, B. & Wilson, E.O. (1990) *Caste and division of labor. The Ants*. Harvard University Press. pp. 301–305.
- Holmgren, N. (1913) Termitenstudien. 4. Versuch einer systematischen Monographie der Termiten der Orientalischen Region. *Kungliga Svenska Vetenskapsakademiens Handlingar*, **50**, 1–276.
- Huang, D., Engel, M.S., Cai, C., Wu, H. & Nel, A. (2012) Diverse transitional giant fleas from the Mesozoic era of China. *Nature*, **483**, 201–204. <https://doi.org/10.1038/nature10839>.
- Huang, D., Nel, A., Cai, C., Lin, Q. & Engel, M.S. (2013) Amphibious flies and paedomorphism in the Jurassic period. *Nature*, **495**, 94–97. <https://doi.org/10.1038/nature11898>.
- Huelsenbeck, J.P. & Ronquist, F. (2001) MRBAYES: Bayesian inference of phylogeny. *Bioinformatics*, **17**, 754–755. <https://doi.org/10.1093/bioinformatics/17.8.754>.

- Invernizzi, E. & Ruxton, G.D. (2019) Deconstructing collective building in social insects: implications for ecological adaptation and evolution. *Insectes Sociaux*, **66**, 507–518. <https://doi.org/10.1007/s00040-019-00719-7>.
- Inward, D. J., Vogler, A. P. & Eggleton, P. (2007) A comprehensive phylogenetic analysis of termites (Isoptera) illuminates key aspects of their evolutionary biology. *Molecular Phylogenetics and Evolution*, **44**, 953–967. <https://doi.org/10.1016/j.ympev.2007.05.014>.
- Kambhampati, S., Kjer, K.M. & Thorne, B.L. (1996) Phylogenetic relationship among termite families based on DNA sequence of mitochondrial 16S rRNA gene. *Insect Molecular Biology*, **5**, 229–238. <https://doi.org/10.1111/j.1365-2583.1996.tb00097.x>.
- Keating, J.N., Sansom, R.S., Sutton, M.D., Knight, C.G. & Garwood, R.J. (2020) Morphological phylogenetics evaluated using novel evolutionary simulations. *Systematic Biology*, **69**, 897–912. <https://doi.org/10.1093/sysbio/syaa012>.
- King, B. & Beck, R.M.D. (2020) Tip dating supports novel resolutions of controversial relationships among early mammals. *Proceedings of the Royal Society (B)*, **287**, 20200943. <http://doi.org/10.1098/rspb.2020.0943>.
- Kosmoswska-Ceranowicz, B., Kohlman-Adamska, A. & Grabowska, I. (1997) Erste Ergebnisse zur Lithologie und Palynologie der Bernstein- führenden Sedimente im Tagebau Primorskoje. *Metalla*, **66**, 5–17.
- Koch, A.L., Frost, F. & Trujillo, K.C. (2006) Paleontological discoveries at Curecanti National Recreation Area and Black Canyon of the Gunnison National Park, Upper Jurassic Morrison Formation, Colorado. In: Foster, J.R. & Lucas, S.G. (eds). Paleontology and Geology of the Upper Jurassic Morrison Formation. *New Mexico Museum of Natural History and Science Bulletin*, **36**, 35–38.
- Krishna, K., Grimaldi, D.A., Krishna, V. & Engel, M.S. (2013) Treatise on the Isoptera of the world. *Bulletin of the American Museum of Natural History*, **377**, 1–2704. <http://hdl.handle.net/2246/6430>.

- Latreille, P.A. (1802) Histoire naturelle, générale et particulière des Crustacés et des Insectes. Ouvrage faisant suite aux œuvres de Leclerc de Buffon et partie du cours complet d'Histoire naturelle rédigé par C.S. Sonnini. T. 3-4, an X. Familles naturelles et genres. Paris, Dufart, 1–467 and 1–387.
- Latreille, P.A. (1810) Histoire naturelle, générale et particulière des Crustacés et des Insectes. Ouvrage faisant suite aux œuvres de Leclerc de Buffon et partie du cours complet d'Histoire naturelle rédigé par C.S. Sonnini. T. 13, an XIII. Familles naturelles et genres. Paris, Dufart, 1–432.
- Legendre, F., Whiting, M. F., Bordereau, C., Canello, E. M., Evans, T. A. & Grandcolas, P. (2008) The phylogeny of termites (Dictyoptera: Isoptera) based on mitochondrial and nuclear markers: implications for the evolution of the worker and pseudergate castes, and foraging behaviors. *Molecular Phylogenetics and Evolution*, **48**, 615–627. <https://doi.org/10.1016/j.ympev.2008.04.017>.
- Legendre F., Whiting M.F. & Grandcolas P. (2013). Phylogenetic analyses of termite post-embryonic sequences illuminate caste and developmental pathway evolution. *Evolution & Development*, **15**, 146–157. <https://doi.org/10.1111/ede.12023>.
- Legendre, F., Nel, A., Svenson, G.J., Robillard, T., Pellens, R. & Grandcolas, P. (2015) Phylogeny of Dictyoptera: dating the origin of cockroaches, praying mantises and termites with molecular data and controlled fossil evidence. *PLoS ONE*, **10**, e0130127. <https://doi.org/10.1371/journal.pone.0130127>.
- Lepage, T., Bryant, D., Philippe, H. & Lartillot, N. (2007) A general comparison of relaxed molecular clock models. *Molecular Biology and Evolution*, **24**, 2669–2680. <https://doi.org/10.1093/molbev/msm193>.
- Lewis, P.O. (2001) A likelihood approach to estimating phylogeny from discrete morphological character data. *Systematic Biology*, **50**, 913–925. <https://doi.org/10.1080/106351501753462876>

- Lin, N. & Michener, C.D. (1972) Evolution of sociality in insects. *The Quarterly Review of Biology*, **47**, 131–159. <https://www.jstor.org/stable/2821773>.
- Luo, A., Duchêne, D.A., Zhang, C., Zhu, C.-D. & Ho, S.-Y. (2020) A simulation-based evaluation of tip-dating under the fossilized birth–death process. *Systematic Biology*, **69**, 325–344. <https://doi.org/10.1093/sysbio/syz038>.
- Luo, Z.-X. (2007) Transformation and diversification in early mammal evolution. *Nature*, **450**, 1011–1019. <https://doi.org/10.1038/nature06277>.
- Luo, Z.-X. & Wible, J.R. (2005) A Late Jurassic digging mammal and early mammalian diversification. *Science*, **308**, 103–107. <https://doi.org/10.1126/science.1108875>.
- Maddison, W.P. & Maddison, D.R. (2019) Mesquite: a modular system for evolutionary analysis. Version 3.61. <http://www.mesquiteproject.org>.
- Martínez-Delclòs, X. & Martinell, J. (1995) The oldest known record of social insects. *Journal of Paleontology*, **69**, 594–599. <https://doi.org/10.1017/S0022336000034983>.
- Michener, C.D. (1974) *The social behavior of the bees: a comparative study*. Cambridge: Harvard University Press, 404 pp.
- Miller, M.A., Pfeiffer, W. & Schwartz, T. (2010) Creating the CIPRES Science Gateway for inference of large phylogenetic trees. Proceedings of the Gateway Computing Environments Workshop (GCE), 14 Nov. 2010, New Orleans, LA, 1–8.
- Mizumoto, N. & Bourguignon, T. (2020) Modern termites inherited the potential of collective construction from their common ancestor. *Ecology and Evolution*, **10**, 6775–6784. <https://doi.org/10.1002/ece3.6381>.
- Moreau, C.S., Bell, C.D., Vila, R., Archibald, S.B. & Pierce, N.E. (2006) Phylogeny of the ants: diversification in the age of angiosperms. *Science*, **312**, 101–104. <https://doi.org/10.1126/science.1124891>.

- Moreau, C.S. & Bell, C.D. (2013) Testing the museum versus cradle tropical biological diversity hypothesis: phylogeny, diversification, and ancestral biogeographic range evolution of the ants. *Evolution*, **67**, 2240–2257. <https://doi.org/10.1111/evo.12105>.
- Nauer, P.A., Hutley, L.B. & Arndt, S.K. (2018) Termite mounds mitigate half of termite methane emissions. *Proceedings of the National Academy of Sciences of the USA*, **115**, 13306–13311. <https://doi.org/10.1073/pnas.1809790115>.
- Nel, A. & Paicheler, J.-C. (1993) Les Isoptera fossiles (Insecta, Dictyoptera). Cahiers de Paléontologie, CNRS (ed.), Paris, 102–179.
- Nel, P., Bertrand, S. & Nel, A. (2018) Diversification of insects since the Devonian: a new approach based on morphological disparity of mouthparts. *Scientific Reports*, **8**, 1–10. <https://doi.org/10.1038/s41598-018-21938-1>.
- Nicholson, D. B., Mayhew, P. J., & Ross, A. J. (2015) Changes to the fossil record of insects through fifteen years of discovery. *PLoS One*, **10**(7), e0128554. <https://doi.org/10.1371/journal.pone.0128554>.
- O'Reilly, J. E., Puttick, M. N., Parry, L., Tanner, A. R., Tarver, J. E., Fleming, J., Pisani, D. & Donoghue, P. C. (2016) Bayesian methods outperform parsimony but at the expense of precision in the estimation of phylogeny from discrete morphological data. *Biology Letters*, **12**, 20160081. <https://doi.org/10.1098/rsbl.2016.0081>.
- Parham, J. F., Donoghue, P. C., Bell, C. J., Calway, T. D., Head, J. J., Holroyd, P. A., Inoue, J. G., Irmis, R. B., Joyce, W. G., Ksepka, D. T., Patané, J. S. L., Smith, N. D., Tarver, J. E., van Tuinen, M., Yang, Z., Angielczyk, K. D., Greenwood, J. M., Hipsley, C. A., Jacobs, L., Makovicky, P. J., Müller, J., Smith, K. T., Theodor, J. M., Warnock, R. C. M., Benton, M. J. (2012) Best practices for justifying fossil calibrations. *Systematic Biology*, **61**(2), 346-359. <https://doi.org/10.1093/sysbio/syr107>.
- Perrichot, V. (2019) New Cretaceous records and the diversification of crown-group ants (Hymenoptera: Formicidae). In: Nascimbene, P.C. (ed.), Abstract book of the 8th International Conference on Fossil Insects, Arthropods & Amber, Santo Domingo, Dominican Republic, p. 66.

- Puttick, M.N., O'Reilly, J.E., Tanner, A.R., Fleming, J.F., Clark, J., Holloway, L., Lozano-Fernandez, J., Parry, L.A., Tarver, J.E., Pisani, D. & Donoghue, P.C. (2017) Uncertain-tree: discriminating among competing approaches to the phylogenetic analysis of phenotype data. *Proceedings of the Royal Society (B) Biological Sciences*, **284** (20162290). <https://doi.org/10.1098/rspb.2016.2290>.
- Pyron, R.A. (2011) Divergence time estimation using fossils as terminal taxa and the origins of Lissamphibia. *Systematic Biology*, **60**, 466–481. <https://doi.org/10.1093/sysbio/syr047>.
- Rambaut, A. (2009) FigTree v1.4.4. Available via <http://tree.bio.ed.ac.uk/software/figtree/>. Accessed March 1, 2020.
- Rambaut, A., Drummond, A.J., Xie, D., Baele, G. & Suchard, M.A. (2018) Posterior summarisation in Bayesian phylogenetics using Tracer 1.7. *Systematic Biology*, **67**, 901–904. <https://doi.org/10.1093/sysbio/syy032>.
- Ronquist, F. & Huelsenbeck, J.P. 2003. MrBayes 3: Bayesian phylogenetic inference under mixed models. *Bioinformatics*, **19**, 1572–1574. <https://doi.org/10.1093/bioinformatics/btg180>.
- Ronquist, F., Klopfstein, S., Vilhelmsen, L., Schulmeister, S., Murray, D.L. & Rasnitsyn, A.P. (2012) A total-evidence approach to dating with fossils, applied to the early radiation of the Hymenoptera. *Systematic Biology*, **61**, 973–999. <https://doi.org/10.1093/sysbio/sys058>.
- Ronquist, F., Lartillot, N. & Phillips, M.J. (2016) Closing the gap between rocks and clocks using total-evidence dating. *Philosophical Transactions of the Royal Society (B) Biological Sciences*, **371** (20150136). <https://doi.org/10.1098/rstb.2015.0136>.
- Ronquist, F., Teslenko, M., van der Mark, P., Ayres, D.L., Darling, A., Höhna, S., Larget, B., Liu, L., Suchard, M.A. & Huelsenbeck, J.P. (2012) MRBAYES 3.2: Efficient Bayesian phylogenetic inference and model selection across a large model space. *Systematic Biology*, **61**, 539–542. <https://doi.org/10.1093/sysbio/sys029>.
- Sadowski, E.M., Schmidt, A.R., Seyfullah, L.J. & Kunzmann, L. (2017) Conifers of the “Baltic amber forest” and their palaeoecological significance. *Stapfia*, **106**, 1–73.

- Scheffrahn, R.H. & Su, N.-Y. (1995) A new subterranean termite introduced to Florida: *Heterotermes* Froggatt (Rhinotermitidae: Heterotermitinae) established in Miami. *Florida Entomologist*, **78**, 623–627. <https://doi.org/10.2307/3496052>.
- Selden, P.A., Shih, C. & Ren D. (2011) A golden orb-weaver spider (Araneae: Nephilidae: Nephila) from the Middle Jurassic of China. *Biology Letters*, **7**, 775–778. <https://doi.org/10.1098/rsbl.2011.0228>.
- Shi, G.H., Grimaldi, D.A., Harlow, G.E., Wang, J., Wang, J., Yang, M.C., Lei, W.Y., Li, Q.L. & Li, X.H. (2012) Age constraint on Burmese amber based on U-Pb dating of zircons. *Cretaceous Research*, **37**, 155–163. <https://doi.org/10.1016/j.cretres.2012.03.014>.
- Simões, T.R., Caldwell, M.W. & Pierce, S.E. (2020) Sphenodontian phylogeny and the impact of model choice in Bayesian morphological clock estimates of divergence times and evolutionary rates. *BMC Biology* **18**, 191. <https://doi.org/10.1186/s12915-020-00901-5>.
- Singh, K., Muljadi, B.P., Raeini, A.Q., Jost, C., Vandeginste, V., Blunt, M.J., Theraulaz, G. & Degond, P. (2019) The architectural design of smart ventilation and drainage systems in termite nests. *Science Advances*, **5** (eaat8520), 1–11. <https://doi.org/10.1126/sciadv.aat8520>.
- Smith, E.M., Loewen, M.A. & Kirkland, J.I. (2020) New social insect nests from the Upper Jurassic Morrison Formation of Utah. *Geology of the Intermountain West*, **7**, 281–299. <https://doi.org/10.31711/giw.v7.pp281-299>.
- Snyder, T.E. (1928) A new *Reticulitermes* from Baltic Sea amber (Insecta Isoptera). *Journal of the Washington Academy of Sciences*, **18**, 515–517. <https://www.jstor.org/stable/24528302>.
- Stadler, T. (2010) Sampling-through-time in birth-death trees. *Journal of Theoretical Biology*, **267**, 396–404. <https://doi.org/10.1016/j.jtbi.2010.09.010>.
- Swofford, D.L. (2002) PAUP: Phylogenetic Analysis Using Parsimony (and Other Methods), Version 4.0 Beta 10. Sinauer Associates, Sunderland.

- Thompson, G.J., Kitade, O., Lo, N. & Crozier, R.H. (2000) Phylogenetic evidence for a single, ancestral origin of a ‘true’ worker caste in termites. *Journal of Evolutionary Biology*, **13**, 869–881. <https://doi.org/10.1046/j.1420-9101.2000.00237.x>.
- Toussaint, E. F., & Condamine, F. L. (2016) To what extent do new fossil discoveries change our understanding of clade evolution? A cautionary tale from burying beetles (Coleoptera: *Nicrophorus*). *Biological Journal of the Linnean Society*, **117**, 686–704. <https://doi.org/10.1111/bij.12710>.
- Vrsansky, P. (2002) Origin and the early evolution of mantises. *AMBA Projekty*, **6**, 1–16.
- Wappler, T. & Engel, M.S. (2006) A new record of *Mastotermes* from the Eocene of Germany (Isoptera: Mastotermitidae). *Journal of Paleontology*, **80**, 380–385. [https://doi.org/10.1666/0022-3360\(2006\)080\[0380:ANROMF\]2.0.CO;2](https://doi.org/10.1666/0022-3360(2006)080[0380:ANROMF]2.0.CO;2).
- Ware, J.L., Grimaldi, D.A. & Engel, M.S. (2010) The effects of fossil placement and calibration on divergence times and rates: an example from the termites (Insecta: Isoptera). *Arthropod Structure & Development*, **39**, 204–219. <https://doi.org/10.1016/j.asd.2009.11.003>.
- Weitschat, W. & Wichard, W. (2010) Baltic amber. In: Penney, D. (Ed.), Biodiversity of fossils in amber from the major world deposits. Siri Scientific Press, Manchester, UK, pp. 80–115.
- Wilson, E.O. (1971) *The Insect societies*. Cambridge: Harvard University Press, 562 pp.
- Wilson, E.O. (1975) *Sociobiology: the new synthesis*. Cambridge: Harvard University Press, 697 pp.
- Wilson E.O. & Hölldobler B. (2005) Eusociality: origin and consequences. *Proceedings of the National Academy of Sciences of the United States of America*, **102**, 13367–13371. <https://doi.org/10.1073/pnas.0505858102>.
- Wright, A.M. (2019) A systematist’s guide to estimating Bayesian phylogenies from morphological data. *Insect Systematics and Diversity*, **3**, 1–14. <https://doi.org/10.1093/isd/ixz006>.
- Wright, A.M. & Hillis, D.M. (2014) Bayesian analysis using a simple likelihood model outperforms parsimony for estimation of phylogeny from discrete morphological data. *PLoS One*, **9** (10), e109210. <https://doi.org/10.1371/journal.pone.0109210>.

- Wu, L-W., Bourguignon, T., Šobotník, J., Wen, P., Liang, W-R. & Li, H-F. (2018) Phylogenetic position of the enigmatic termite family Stylotermitidae (Insecta: Blattodea). *Invertebrate Systematics*, **32**, 1111–1117. <https://doi.org/10.1071/IS17093>.
- Yu, T., Kelly, R., Mu, L., Ross, A., Kennedy, J., Broly, P., Xia, F., Zhang, H., Wang, B. & Dilcher, D. (2019) An ammonite trapped in Burmese amber. *Proceedings of the National Academy of Sciences of the United States of America*, **116**, 11345–11350. <https://doi.org/10.1073/pnas.1821292116>.
- Zhang, C., Stadler, T., Klopfstein, S., Heath, T. A., & Ronquist, F. (2016) Total-evidence dating under the fossilized birth–death process. *Systematic Biology*, **65**, 228–249. <https://doi.org/10.1093/sysbio/syv080>.
- Zhang, C. & Wang, M. (2019) Bayesian tip dating reveals heterogeneous morphological clocks in Mesozoic birds. *Royal Society Open Science*, **6**, 182062. <http://doi.org/10.1098/rsos.182062>.
- Zhao, Z., Eggleton, P., Yin, X., Gao, T., Shih, C. & Ren, D. (2019) The oldest known mastotermitids (Blattodea: Termitoidea) and phylogeny of basal termites. *Systematic Entomology*, **44**, 612–623. <https://doi.org/10.1111/syen.12344>.
- Zhao, Z., Yin, X., Shih, C., Gao, T. & Ren, D. (2020a) Termite colonies from mid-Cretaceous Myanmar demonstrate their early eusocial lifestyle in damp wood. *National Science Review*, **7**, 381–390. <https://doi.org/10.1093/nsr/nwz141>.
- Zhao, Z., Shih, C., Gao, T. & Ren, D. (2020b) Termite communities and their early evolution and ecology trapped in Cretaceous amber. *Cretaceous Research*, **117**, 104612. <https://doi.org/10.1016/j.cretres.2020.104612>.

Figure captions:

**Fig. 1.** *Milesitermes engeli* gen. et sp. nov., holotype IGR.BU-012. Photographs. (A) habitus in dorsal view; (B) detailed view of mouthparts; (C) detailed view of terminalia (black arrows cerci

segmentation). Mxp: maxillary palp; Mdb: mandibles; Lb: labial palp; Lci: lacinial incisor; Prg: paraglossa; Gl: galea. Scale bars 0.5 mm.

**Fig. 2.** *Milesitermes engeli* **gen. et sp. nov.**, holotype IGR.BU-012. Reconstruction drawings. (A) dorsal view; (B); apex of fore legs; (C) apex of mid-legs; (D) apex of hind-legs. Scale bars 0.5 mm (A); 0.25 mm (B–D).

**Fig. 3.** *Reticulitermes grimaldii* **sp. nov.**, holotype IGR.BA-020 (A) photographs. Habitus in ventro-lateral view. (B) detailed view of mouthparts; (C) detailed view of antenna; (D) detailed view of terminalia (black arrows cerci, red arrows styli). Scale bars 0.5mm (a); 0.25 mm (B–D).

**Fig. 4.** *Reticulitermes grimaldii* **sp. nov.**, holotype IGR.BA-020. Reconstruction drawings. (A) habitus in ventro-lateral view; (B) Apex of protibiae; (C) apex of mid-tibiae; (d) apex of hind legs. Scale bars 0.5 mm (A); 0.25 mm (B–D)

**Fig. 5.** Dated-tree recovered from a FBD model analysis with a single partition (Script\_FBD-1part), combining extant and extinct species, with a birth-death serial sampling (no sampled ancestor allowed) and uniform fossil calibrations. Bars at each node represent 95 % HPD in dating estimates. Dotted square represent crown-lineages. LT = Late Triassic, Pal = Paleocene, Oligo = Oligocene, Mio = Miocene, P = Pliocene-Pleistocene.

**Fig. 6.** Dated-trees recovered from Bayesian analyses. (A) node-dating (Script\_node-dating), only extant species, single partition, birth-death tree prior and diversity sampling; (B) FBD model with three partitions (script\_FBD-3part), including extant and extinct species, with a birth-death serial sampling (no sampled ancestor allowed) and uniform fossil calibrations. Branches are colored according to the relative rates of change for the ‘alates/workers’ partition. LT = Late Triassic, Pli = Pliocene, Ple = Pleistocene.

**Fig. 7.** Dated-trees recovered from Bayesian analyses. FBD model with three partitions (script\_FBD-3part), including extant and extinct species, with a birth-death serial sampling (no sampled ancestor allowed) and uniform fossil calibrations (i.e. same tree as in Fig 6B). Branches are colored according to the relative rates of change for the ‘soldier’ (a) and ‘biology’ partitions (b).

**Table 1.** Date estimates (in Ma) for Isoptera and subclades. Age estimates for stem- and crown-groups are distinguished when possible. Estimates are older for Fossilized Birth-Death analyses that include extinct species when compared to the node dating analyses (with only extant species); analyses wherein sampled ancestors are allowed give old estimates and several dubious values for other parameters (see Supporting Information); 144 and 163 Ma correspond to the mean age for Isoptera (150 Ma for other analyses).

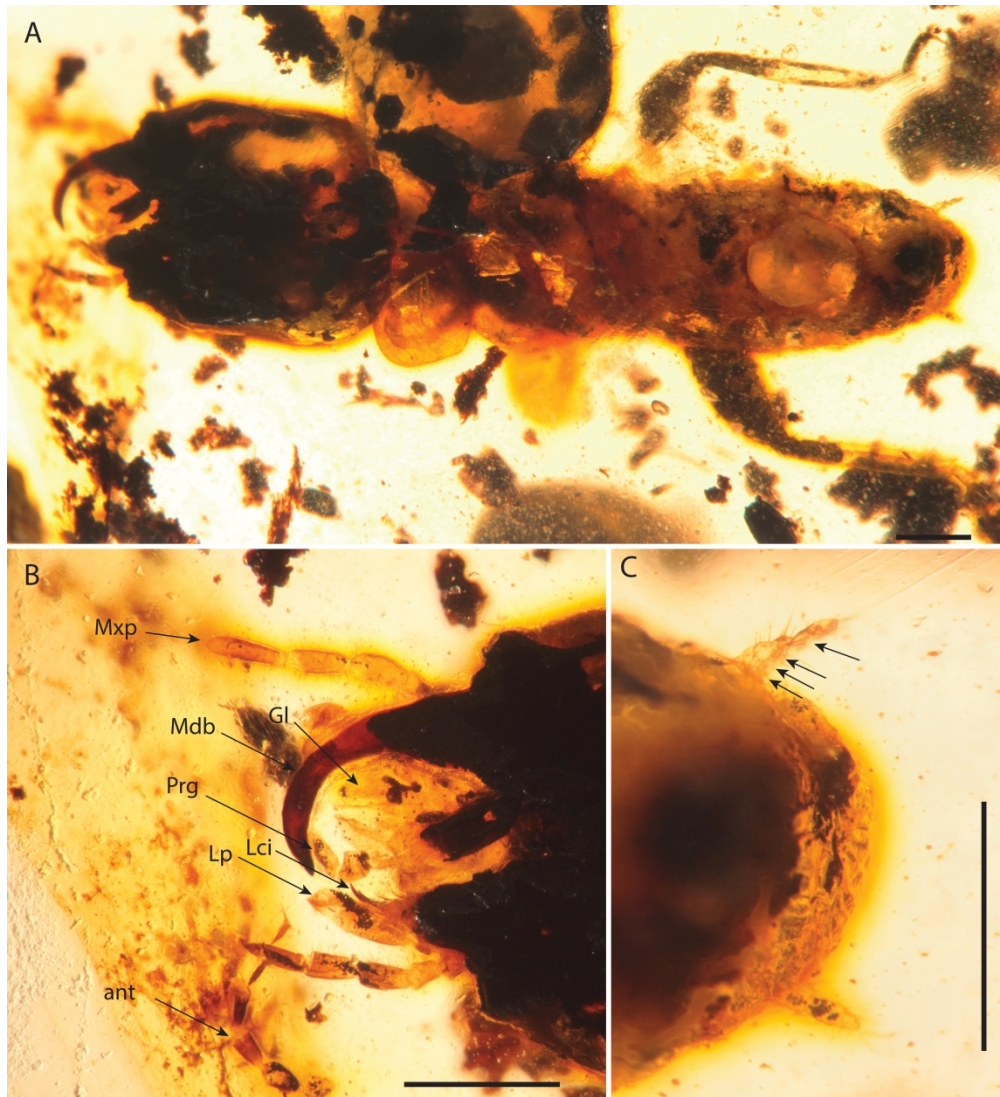


Figure 1

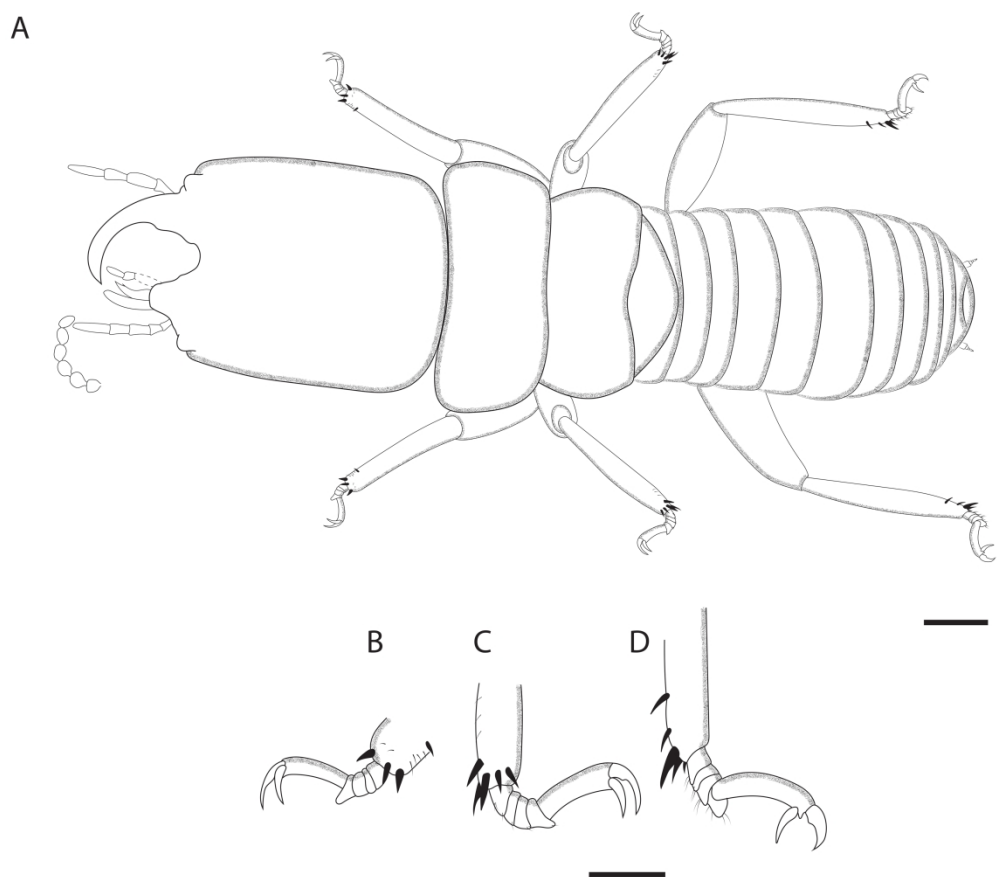


figure 2

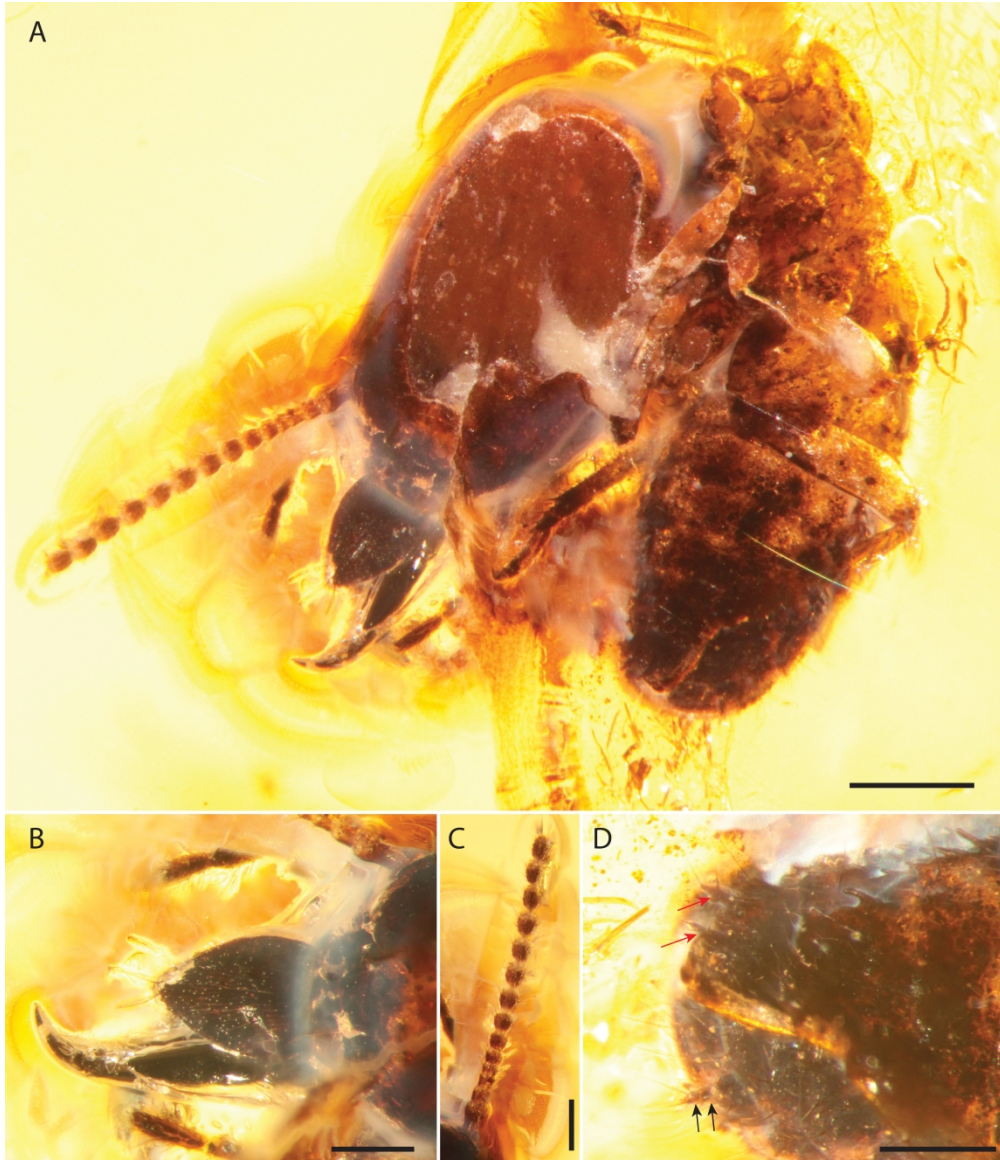


figure 3

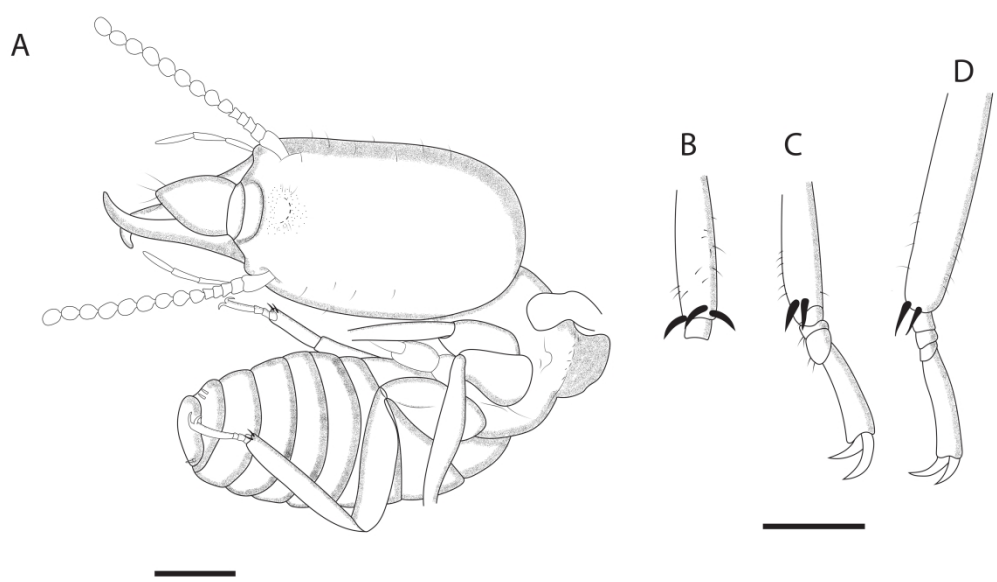


figure 4

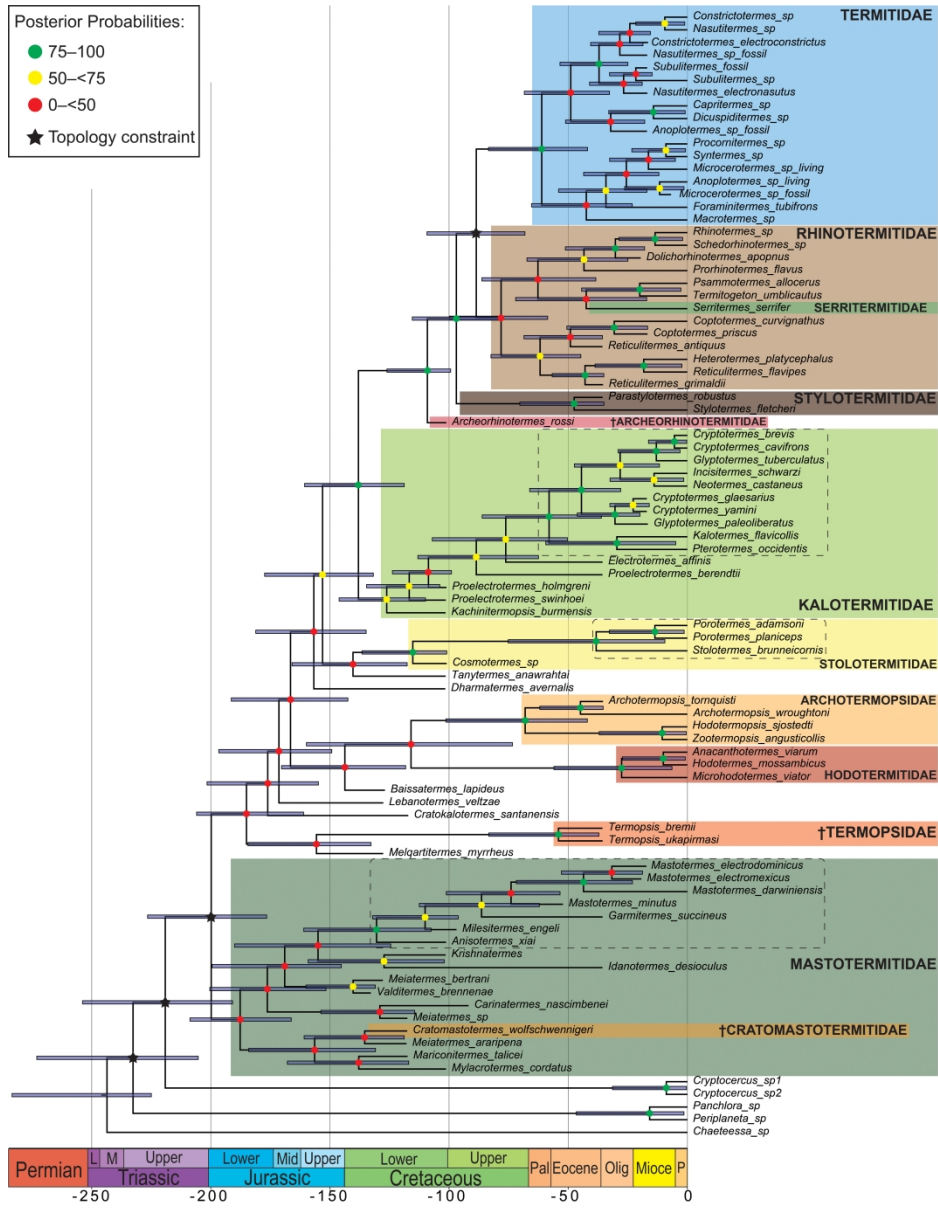


figure 5

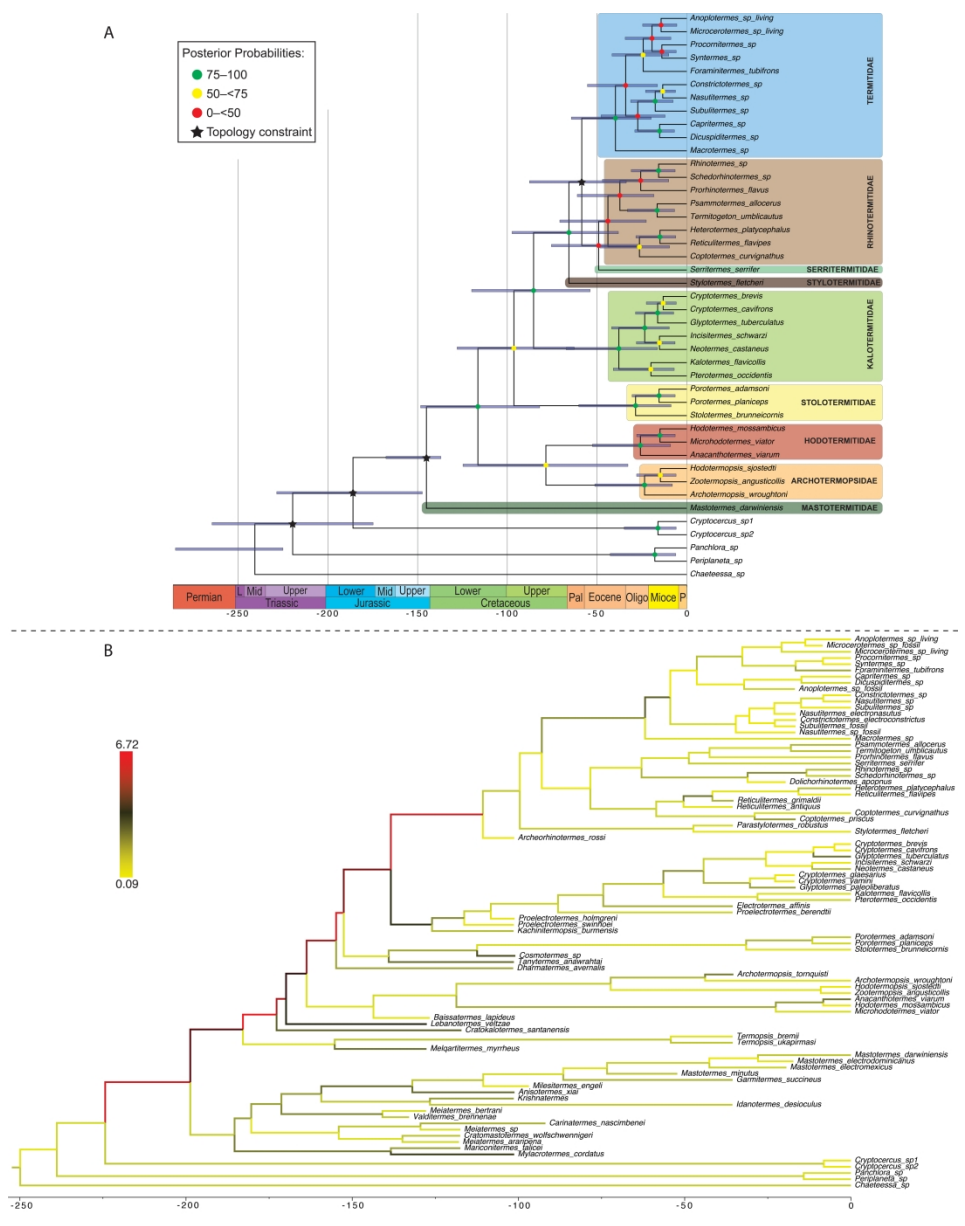


figure 6



	Node dating analyses						
	Node dating		ND-BD-random		ND-uni-random		ND-uni-c
	mean	95%HPD	mean	95%HPD	mean	95%HPD	mean
<b>Stem-Isoptera</b>	186	147-229	188	148 - 229	190	147 - 248	191
<b>Crown-Isoptera</b>	145	137-167	146	137 - 171	143	137 - 163	143
<b>Euisoptera</b>	116	82-149	119	84 - 152	135	119 - 158	135
<b>Neoisoptera</b>	66	38-97	71	41 - 106	109	84 - 134	109
<b>Termopsidae</b>	-	-	-	-	-	-	-
<b>Archotermopsidae</b>	24	9-60	24	3 - 57	46	11 - 92	45
<b>Hodotermitidae</b>	26	9-53	24	5 - 53	47	14 - 90	46
<b>Crown-Stolotermitidae</b>	29	9-60	29	5 - 65	59	20 - 109	59
<b>Stem-Stolotermitidae</b>	96	63-128	101	70 - 137	126	106 - 150	127
<b>Crown-Kalotermitidae</b>	38	16-67	38	15 - 72	75	41 - 112	75
<b>Stem-Kalotermitidae</b>	85	54-120	91	60 - 127	120	97 - 144	120
<b>Crown-Termitidae</b>	40	20-64	42	19 - 70	78	51 - 106	79
<b>Stem-Termitidae</b>	59	34-88	64	35 - 95	103	79 - 128	102

diversity 95%HPD	One partition (1p)		1p – 144 Ma		1p – 163 Ma		Three part
	mean	95%HPD	mean	95%HPD	mean	95%HPD	mean
148 - 252	219	191-254	212	187-243	223	195-262	224
137 - 163	200	177-227	191	171-213	206	180-234	199
118 - 157	185	161-206	177	156-198	188	164-213	183
84 - 134	109	99-126	108	99-123	109	99-127	111
-	54	37-83	54	37-81	55	37-85	54
11 - 92	68	42-101	67	43-100	68	43-104	72
13 - 88	28	6-56	27	6-54	28	7-56	23
18 - 107	38	9-75	36	9-73	39	10-77	32
107 - 151	115	101-137	114	101-134	115	100-137	112
40 - 111	58	36-86	56	34-82	58	36-86	56
98 - 144	126	110-146	125	110-144	128	111-149	126
51 - 106	61	42-83	59	41-81	62	42-84	62
78 - 127	89	68-109	86	66-106	89	68-110	93

Fossilized Birth-Death process analyses							
titions (3p)	3p and rate variable		One partition (1p-equal)		1p-flatpriors		1p-fixed-d
	95%HPD	mean	95%HPD	mean	95%HPD	mean	95%HPD
196-265	224	193-263	223	196-257	219	191 - 254	194
177-224	198	176-225	205	182-229	200	177 - 225	177
162-203	188	168-216	183	158-208	183	160 - 206	161
100-129	111	99-129	114	100-133	109	99 - 126	99
37-84	54	38-82	59	37-85	54	37 - 84	40
47-106	72	46-106	73	43-105	68	43 - 102	38
5-46	23	5-46	32	9-61	28	6 - 57	6
8-84	32	8-65	43	12-81	39	10 - 77	7
101-130	112	101-130	118	101-138	115	101 - 136	109*
36-81	57	36-82	62	37-86	58	37 - 86	24*
111-145	126	110-146	130	112-151	126	109 - 146	111
44-82	61	44-82	64	43-86	62	42 - 83	25
73-113	93	73-115	92	71-115	89	69 - 109	51

diversity 95%HPD	1p-fixed-fossiltip		1p-fixed-random		1p-uni-diversity		1p-uni-random	
	mean	95%HPD	mean	95%HPD	mean	95%HPD	mean	95%HPD
172 - 221	216	188 - 251	258	216 - 309	254	215 - 299	274	228 - 325
172 - 221	196	173 - 222	224	196 - 256	223	198 - 252	236	207 - 270
145 - 178	181	157 - 207	200	173 - 232	193	168 - 226	211	180 - 245
98 - 104	105	98 - 121	101	98 - 110	104	98 - 113	105	99 - 116
35 - 50	52	35 - 80	46	35 - 64	47	37 - 64	49	37 - 68
34 - 49	65	42 - 99	64	41 - 91	64	44 - 91	68	44 - 98
2 - 13	26	7 - 55	19	7 - 36	20	10 - 34	20	7 - 37
2 - 14	37	10 - 74	21	7 - 43	22	10 - 41	23	7 - 46
99 - 124	112	98 - 131	110	98 - 129	113	100 - 130	115	101 - 135
16 - 35	55	33 - 81	42	27 - 60	41	27 - 58	47	30 - 67
102 - 123	122	106 - 142	124	107 - 144	126	110 - 145	129	111 - 151
19 - 33	57	39 - 78	41	29 - 55	41	30 - 55	46	33 - 61
41 - 65	85	65 - 106	77	60 - 93	77	62 - 95	82	66 - 100

<b>1p-clock_uni</b>		
<b>mean</b>	<b>95%HPD</b>	
274	204 - 362	
215	180 - 257	
205	177 - 243	
163	128 - 204	
73	39 - 122	
95	54 - 151	
50	12 - 101	
72	20 - 125	
133	104 - 174	
101	62 - 146	
160	127 - 199	
117	79 - 156	
150	113 - 192	



	<b>Character</b>
1	Number of antennomeres in alate/imago
2	Structure of imago flagellum
3	Apex of imago flagellum
4	Ocelli of alates
5	Ocelli of soldiers
6	Pigmentation of soldier compound eyes
7	Soldier compound eyes
8	Frontal gland developed into a distinct fontanelle
9	Position of alate head
10	Ventral cervical sclerite of alate
11	Marginal teeth of left mandible of alate
12	Subsidiary tooth of right mandible of alate
13	Lacinial teeth of maxilla
14	Postclypeal furrow (workers and alates)
15	Clypeus (worker only) in profile
16	Shape of occipital foramen in imago
17	Y-shaped coronal ecdysial cleavage line in imago
18	Pair of ocellus-like structures (five ocelloids) near inner margin of compound eye
19	Occipital sulcus
20	Compound eye
21	Notch between first and third marginal teeth
22	Mandibular excavation between apical and first marginal teeth
23	Soldier mandible: marginal teeth
24	Soldier mandible
25	Soldier mandible
26	Soldier head capsule
27	Diagonal grooves between fontanelle and postclypeus
28	Pronotal posterolateral corners of imago
29	Pronotal posterior margin of imago
30	Pronotal lateral margins of imago
31	Pronotal size of imago
32	Pronotal anterior margin of imago
33	Tibial macrosetae and spurs
34	Tibial macrosetae and spurs
35	Tarsomeres
36	Metabasitarsomere length
37	Pretarsal arolium
38	Plantular pads
39	Procoxal ventral keel of alate
40	Protibial spines along length
41	Forewing first Rs fork
42	Forewing length of R1
43	Forewing Rs
44	Forewing CuA
45	Multiple branches of R1
46	Forewing tegmenization
47	Wings
48	Forewing vein M
49	Forewing scale relative to hind wing scale
50	Wing membrane setae
51	Fore- and hind wings
52	Forewing basal cleavage suture
53	Hind wing basal cleavage suture

54	Crossveins connecting longitudinal veins
55	Sclerotization of veins
56	Anal lobe of hind wing
57	Hind wing vein A1
58	Wing membrane reticulations
59	Wing membrane surface
60	Radial fracture of forewing scale
61	Reticulation between CuA and CuP on forewing scale
62	Distal margin of forewing scale
63	CuP in forewing scale
64	Humeral margin of forewing scale
65	Forewing CuP
66	Position of forewing vein M
67	Costalization of forewing
68	Branches of Rs
69	Branches of vein M
70	Radial area
71	Development of CuP
72	Dichotomous branching of R and M
73	Number of superior branches of Rs
74	Female styli
75	Imago cercus segmentation
76	Castes
77	Ootheca
78	Presence of Blattabacterium in fat body
79	Presence of flagellates and ciliates
80	Wood feeding
81	Social organization
82	Living in structures/nests
83	Soldiers
84	Soldier nasus
85	Nasute fontanelle
86	First proctodeal segment
87	Soldier labral apex
88	Soldier heads
89	Soldier labrum
90	Soldier pronotum
91	Malpighian tubule number
92	Imago/worker fontanelle
93	Anterior margin of worker/alate postclypeus
94	Imago compound eyes
95	Imago ocelloid
96	Soldier fontanelle
97	Nasute head capsule
98	Proventricular teeth
99	Protibial apical spur number
100	Mesotibial apical spurs
101	Metatibial apical spurs
102	Sternal gland on third sternum
103	Sternal gland on fourth sternum
104	Sternal gland on fifth sternum
105	Soldier labral brush
106	Setulae surrounding fontanelle (directed toward fontanelle)
107	Hind wing vein M
108	Soldier frontal groove
109	Soldier head anterior to vertex

110	Soldier head with lateral striation
111	Soldier head capsule with posterolateral temples

<b>Character-State descriptions</b>
50 or more antennomeres=0; 30-40 antennomeres=1; 23-28 antennomeres=2; 11-22 antennomeres=3
flagellomeres filiform=0; flagellomeres moniliform=1;
distal 7-8 articles tapered=0; distal 7-8 articles not tapered=1;
three present (homologous with other orders)=0; absent=1
present=0; absent=1;
present=0; absent=1;
rudimentary=0; absent=1;
absent=0; present=1
hypo-/orthognathous=0; prognathous=1;
present=0; absent=1
greater than or equal to three=0; two teeth=1;
absent=0; present=1;
both teeth apical=0; one tooth subapical=1;
absent=0; present as shallow longitudinal furrow=1
Not keeled=0; with keel=1
rounded=0; trapezoidal=1
present=0; absent or highly vestigial=1;
present as circular tympanalike areas=0; vestigial as areas of weakened or pale cuticle=1; absent=2; present and nearly lens like (superficially resembling ocelli and historically termed ocelli by isopterists)=3;
present=0; absent or highly vestigial=1;
lenticular=0; circular=1;
present=0; absent=1;
absent=0; present=1;
distributed along length; with 1-4 teeth along middle of margin=0; lost except small teeth/serrations at base=1
short to moderate in length, length ca 2 or less x basal width=0; greatly elongate and narrow, length ca. 3 or more x basal
symmetrical, not clicking=0; asymmetrical, clicking=1
rectangular in dorsal aspect=0; phragmotic, plug shaped=1;
absent=0; present=1;
broadly arched=0; acutely rounded, nearly orthogonal=1;
Straight or slightly indented=0; rounded=1
subparallel=0; converging=1;
covering head dorsally=0; not covering head but with width greater than or equal to head=1; width significantly less than
concave=0; relatively straight=1; convex, with anterolateral corners developed=2;
heavily serrate=0; slightly pimplate=1; smooth=2
asymmetrical, with one side flattened=0; symmetrical=1
pentamerous, fully developed=0; pentamerous, second tarsal article reduced=1; tetramerous (second tarsal article lost)=2;
less than twice the width=0; more than 3 times the width=1; more than twice but less than 3 times=2; (0,1)=3
present=0; absent=1;
present=0; absent=1
present=0; absent=1;
present and extensive=0; absent, reduced to apical spines/spurs=1;
In basal half=0; near mid length or beyond=1
short, extending in quarter of wing length=0; median, extending in third of wing length=1; long, extending to or past wing
branched basally in scale with 2-3 branches=0; simple in scale=1;
shorter, to around wing midlength=0; long, to point within apical third of wing=1; elongate and extensively developed,
present=0; absent=1;
Developed as tegmina=0; not developed as complete tegmina=1
present=0; absent=1;
present=0; absent=1
with apical margin meeting or overlapping hind wing scale=0; scales well separated=1;
absent=0; present, microsetulose=1
not dehiscent=0; dehiscent=1;
absent=0; present=1;
absent=0; present but rudimentary=1; completely developed=2;

present=0; absent=1
all uniformly sclerotized=0; Sc, R, and M thick and sclerotized relative to CuA=1; Sc and R sclerotized relative to M and
present=0; absent (wing homonomous)=1;
present=0; absent=1;
present, not pigmented=0; present, pigmented=1; absent=2
smooth=0; nodulose or pimplate=1;
present=0; absent=1
veins=0; reticulations=1; reticulations only anterior to CuP=2; absent= 3
evenly convex=0; straight to slightly convex=1; straight and diagonal=2;
convex=0; straight or concave=1;
flat=0; swollen beyond level of costal margin=1;
terminates prior to posterior tip of basal suture=0; terminates in basal suture=1;
close to Rs=0; midway between Rs and CuA or closer to latter=1;
not costalized=0; C+Sc+R and Rs extremely close and simple and parallel=1;
with dorsal and ventral branches, inferiors irregular (acute go tip)=0; with dorsal and ventral branches, inferiors angled &
with two or more branches=0; with one apical branch=1; simple (unbranched)=2;
encompassing apex or terminating at apex=0; terminating anterior to apex=1;
extensive, developed as claval furrow=0; reduced, confined to short, simple vein near wing base=1;
extensive=0; reduced=1
none=0; one=1; two=2; three=3; four=4; five=5; six=6; seven or more=7; (3 5 6)=8; (34567)=9
present=0; absent=1;
four or higher=0; three=1; one or two=2;
absent=0; present, with true workers=1; present, without true workers=2;
present=0; absent=1;
present=0; absent=1;
present=0; absent=1;
absent=0; present=1;
absent=0; extended parental care=1; eusocial=2;
absent=0; present=1;
present=0; absent=1;
short=0; very long, length several times width=1
Rimmed or slitlike=1; minute, not rimmed or slitlike=1
expanded=0; tubular, not dilated=1
sclerotized=0; hyaline=1
normal=0; flattened=1;
Well developped=0; vestigial=1
Flat=0; saddle shaped=1
Eight or more=0; four or fewer=1
Small and round=0; slit-,drop-, or Y-shaped=1; (0,1)=2
Flat or concave=0; convex=1
Protruding well beyond lateral margin of head=0; small, not protruding beyond lateral margin of head in frontal view=1
Large, ca. 7-8x of compound eye facet=0; small; ca. 2-3x diameter of compound eye facet=1
Normal, dorsal-facing=0; enlarged and facing antieriad=1
not constricted=0; slightly constricted=1
Present=0; highly reduced or lost=1
three or more=0; two=1;
four or five=0; three=1; two=2;
four=0; three=1; two=2;
present=0; absent=1;
present=0; absent=1;
present=0; absent=1;
absent=0; present=1
absent=0; present=1
present=0; absent=1
absent=0; present (ridges anterior from fontanelle with width of fontanelle)=1
not dorsoventrally flattened=0; flattened=1

absent=0; present=1
---------------------

tapered or rounded=0; greatly produced and lobed=1
--

Species / Prior	Locality	Min	Max / Mean (for prior)
<b>Anoplotermes_sp_fossil</b>	Dominican amber	13.65	20.43
<b>Archeorhinotermes_rossi</b>	Burmese amber	98.0	105.0
<b>Archotermopsis_tomquisti</b>	Baltic amber	33.9	37.2
<b>Baissatermes_lapideus</b>	Baissa formation, Russia	112.6	140.0
<b>Carinatermes_nascimbenei</b>	Raritan amber	89.3	94.3
<b>Constrictotermes_electroconstrictus</b>	Dominican amber	13.65	20.43
<b>Coptotermes_priscus</b>	Dominican amber	13.65	20.43
<b>Cratokalotermes_santanensis</b>	Crato formation	112.6	122.46
<b>Cratomastotermes_wolfschweningeri</b>	Crato formation	112.6	122.46
<b>Cryptotermes_glaesarius</b>	Dominican amber	13.65	20.43
<b>Cryptotermes_yamini</b>	Dominican amber	13.65	20.43
<b>Dharmatermes_avenalis</b>	Burmese amber	98.0	105.0
<b>Dolichorhinotermes_apopnus</b>	Mexican amber	15.97	23.3
<b>Electrotermes_affinis</b>	Baltic amber	33.9	37.2
<b>Garmitermes_succineus</b>	Baltic amber	33.9	37.2
<b>Glyptotermes_paleolibertus</b>	Dominican amber	13.65	20.43
<b>Krishnatermes</b>	Burmese amber	98.0	105.0
<b>Mariconitermes_talicei</b>	Crato formation	112.6	122.46

<b>Mastotermes_electrodominicus</b>	Dominican amber	13.65	20.43
<b>Mastotermes_electromexicus</b>	Mexican amber	15.97	23.3
<b>Mastotermes_minutus</b>	Oise amber	48.6	55.8
<b>Meiatermes_araripena</b>	Crato formation	112.6	122.46
<b>Meiatermes_bertrani</b>	Crato formation	112.6	122.46
<b>Meiatermes_sp</b>	Crato formation	112.6	122.46
<b>Melqartitermes_myrrheus</b>	Jezzine, Lebanese amber	125.45	130.0
<b>Microcerotermes_spp_fossil</b>	Dominican amber	13.65	20.43
<b>Mylacrotermes_cordatus</b>	Burmese amber	98.0	105.0
<b>Nasutitermes_electronasutus</b>	Dominican amber	13.65	20.43
<b>Nasutitermes_spp_fossil</b>	Dominican amber	13.65	20.43
<b>Parastylotermes_robotus</b>	Baltic amber	33.9	37.2
<b>Proelectrotermes_berendtii</b>	Baltic amber	33.9	37.2
<b>Proelectrotermes_holmgreni</b>	Burmese amber	98.0	105.0
<b>Proelectrotermes_swinhoei</b>	Burmese amber	98.0	105.0
<b>Reticulitermes_antiquus</b>	Baltic amber	33.9	37.2
<b>Subulitermes_fossil</b>	Mexican amber	15.97	23.3

<b>Tanytermes_anawrahtai</b>	Burmese amber	98.0	105.0
<b>Termopsis_bremii</b>	Baltic amber	33.9	37.2
<b>Termopsis_ukapirmasi</b>	Baltic amber	33.9	37.2
<b>Valditermes_brennenaë</b>	Lower Weald Clay Member	130.0	136.4
<b>Anisotermes_xiai</b>	Burmese amber	98.0	105.0
<b>Idanotermes_desioliculus</b>	Baltic amber	33.9	37.2
<b>Kachinitermopsis_burmensis</b>	Burmese amber	98.0	105.0
<b>Lebanotermes_veltzae</b>	Amber from Mdeyrj-Hammana, Casa Baabda	125.45	130.0
<b>Cosmotermes_sp</b>	Burmese amber	98.0	105.0
<b>Milestermes_engeli</b>	Burmese amber	98.0	105.0
<b>Reticulitermes_griemaldii</b>	Baltic amber	33.9	37.2

Justification
<p>Dominican amber is mined from several deposit dated from the Langhian-Burdigalian ( Iturrealde-Vincent &amp; MacPhee, 1996; Seyfullah <i>et al.</i>, 2018). Due to the lack of information concerning the exact provenance of the amber we do not constrain to precisely the age of taxa derivating from this deposit</p>
<p>Radiometric data established an early Cenomanian age (<math>98.79 \pm 0.62</math> Ma) while some ammonites found in the amber-bearing bed and within amber corroborate a late Albian / early Cenomanian age (Cruickshank &amp; Ko, 2003; Yu <i>et al.</i>, 2019). We use the minimum age recovered from zircon and a mid-Albian age allowing errors due to the <del>older stratigraphic levels currently mined and where the amber pieces might have</del></p>
<p>Blue Earth Formation was dated as late Bartonian to Priabonian (upper Eocene, ca. 33.9–37.2 Ma) based on palynological data (Kosmoswska-Ceranowicz <i>et al.</i>, 1997; Aleksandrova &amp; Zaporozhets, 2008).</p>
<p>Most paleozoologists assign the Zaza Formation to the Neocomian, most probably Berriasian (Rasnitsyn <i>et al.</i>, 1998). However, the presence of <i>Asteropollenites lead</i> palynologists and paleobotanists to believe that the Baissa deposits are younger, possibly Aptian (Vakhrameev &amp; Kotova, 1997). In any case, the faunistic data indicate pre-Aptian. We therefore us the stratigraphic age of former Aptian (when the taxa was</p>
<p>The amber deposit is Turonian age (Doyle &amp; Robbins, 1977; Christopher, 1979) while the base of the Raritan formation is Cenomanian (Brenner, 1967; Cooban &amp; Kennedy,</p>
<p>Dominican amber is mined from several deposit dated from the Langhian-Burdigalian (Seyfullah <i>et al.</i>, 2018; Iturrealde-Vincent &amp; MacPhee, 1996). Due to the lack of information concerning the exact provenance of the amber we do not constrain to precisely the age of taxa derivating from this deposit</p>
<p>Dominican amber is mined from several deposit dated from the Langhian-Burdigalian (Seyfullah <i>et al.</i>, 2018; Iturrealde-Vincent &amp; MacPhee, 1996). Due to the lack of information concerning the exact provenance of the amber we do not constrain to precisely the age of taxa derivating from this deposit</p>
<p>The fossiliferous unit has been dated as Aptian or perhaps early Albian on the basis of its palynology (Pons <i>et al.</i>, 1991) and therefore, we follow the age proposed by <a href="http://fossilworks.org/">http://fossilworks.org/</a></p>
<p>The fossiliferous unit has been dated as Aptian or perhaps early Albian on the basis of its palynology (Pons <i>et al.</i>, 1991) and therefore, we follow the age proposed by <a href="http://fossilworks.org/">http://fossilworks.org/</a></p>
<p>Dominican amber is mined from several deposit dated from the Langhian-Burdigalian (Seyfullah <i>et al.</i>, 2018; Iturrealde-Vincent &amp; MacPhee, 1996). Due to the lack of information concerning the exact provenance of the amber we do not constrain to precisely the age of taxa derivating from this deposit</p>
<p>Dominican amber is mined from several deposit dated from the Langhian-Burdigalian (Seyfullah <i>et al.</i>, 2018; Iturrealde-Vincent &amp; MacPhee, 1996). Due to the lack of information concerning the exact provenance of the amber we do not constrain to precisely the age of taxa derivating from this deposit</p>
<p>Radiometric data established an Early Cenomanian age (<math>98.79 \pm 0.62</math> Ma) while some ammonites found in the amber-bearing bed and within amber corroborate a late Albian / early Cenomanian age (Cruickshank &amp; Ko, 2003; Yu <i>et al.</i>, 2019). We use the minimum age recovered from zircon and a mid-Albian age allowing errors due to the <del>older stratigraphic levels currently mined and where the amber pieces might have</del></p>
<p>Mexican amber-bearing strata extend from the Balumtun Sandstone of the lower Miocene to the La Quinta Formation of the upper Oligocene (Poinar &amp; Brown, 2002). A lower Miocene mid-Oligocene age has been proposed by Berggren &amp; Van Couvering, (1974) while a recent publication proposed a Serravallian-Burdigalian age (Seyfullah <i>et al.</i>, 2018). Therefore we chose a mean age corresponding to the</p>
<p>Blue Earth Formation was dated as late Bartonian to Priabonian (upper Eocene, ca. 33.9–37.2 Ma) based on palynological data (Kosmoswska-Ceranowicz <i>et al.</i>, 1997; Aleksandrova &amp; Zaporozhets, 2008).</p>
<p>Blue Earth Formation was dated as late Bartonian to Priabonian (upper Eocene, ca. 33.9–37.2 Ma) based on palynological data (Kosmoswska-Ceranowicz <i>et al.</i>, 1997; Aleksandrova &amp; Zaporozhets, 2008).</p>
<p>Dominican amber is mined from several deposit dated from the Langhian-Burdigalian (Seyfullah <i>et al.</i>, 2018; Iturrealde-Vincent &amp; MacPhee, 1996). Due to the lack of information concerning the exact provenance of the amber we do not constrain to precisely the age of taxa derivating from this deposit</p>
<p>Radiometric data established an early Cenomanian age (<math>98.79 \pm 0.62</math> Ma) while some ammonites found in the amber-bearing bed and within amber corroborate a late Albian / early Cenomanian age (Cruickshank &amp; Ko, 2003; Yu <i>et al.</i>, 2019). We use the minimum age recovered from zircon and a mid-Albian age allowing errors due to the <del>older stratigraphic levels currently mined and where the amber pieces might have</del></p>
<p>The fossiliferous unit has been dated as Aptian or perhaps early Albian on the basis of its palynology (Pons <i>et al.</i>, 1991) and therefore, we follow the age proposed by <a href="http://fossilworks.org/">http://fossilworks.org/</a></p>

<p>Dominican amber is mined from several deposit dated from the Langhian-Burdigalian (Seyfullah <i>et al.</i>, 2018; Iturralde-Vincent &amp; MacPhee, 1996). Due to the lack of information concerning the exact provenance of the amber we do not constrain to precisely the age of taxa derivating from this deposit</p>
<p>Mexican amber-bearing strata extend from the Balumtun Sandstone of the lower Miocene to the La Quinta Formation of the upper Oligocene (Poinar &amp; Brown, 2002). A lower Miocene mid-Oligocene age has been proposed by Berggren &amp; Van Couvering, (1974) while a recent publication proposed a Serravallian-Burdigalian age (Seyfullah <i>et al.</i>, 2018). Therefore we chose a mean age corresponding to the</p>
<p>Oise amber is dated back from Sparnacian (early Eocene) continental facies (De Franceschi &amp; De Ploëg, 2003)</p>
<p>The fossiliferous unit has been dated as Aptian or perhaps early Albian on the basis of its palynology (Pons <i>et al.</i>, 1991) and therefore, we follow the age proposed by <a href="http://fossilworks.org/">http://fossilworks.org/</a></p>
<p>The fossiliferous unit has been dated as Aptian or perhaps early Albian on the basis of its palynology (Pons <i>et al.</i>, 1991) and therefore, we follow the age proposed by <a href="http://fossilworks.org/">http://fossilworks.org/</a></p>
<p>The fossiliferous unit has been dated as Aptian or perhaps early Albian on the basis of its palynology (Pons <i>et al.</i>, 1991) and therefore, we follow the age proposed by <a href="http://fossilworks.org/">http://fossilworks.org/</a></p>
<p>Amber found in three intervals in the upper part of the Grès du Liban. Hammana is found in the upper interval, located between the Jezzian above and the "Banc de Mrejatt" below. The "Banc de Mrejatt" includes one biostratigraphically significant benthic foraminifer: <i>Eopalarbitolina transiens</i> (Cherchi &amp; Schroeder, 1999), which is a zonal marker of the lower to upper Barremian transition according to Schroeder <i>et al.</i> (2010). Accordingly the "Banc de Mrejatt" is correlated to the transgression of sequence Ba3 of Clavel <i>et al.</i> (2007) and ascribed a late early Barremian age. The lower subunit is assigned a late Barremian age although the amber may be reworked</p>
<p>Dominican amber is mined from several deposit dated from the Langhian-Burdigalian ( Iturralde-Vincent &amp; MacPhee, 1996; Seyfullah <i>et al.</i>, 2018). Due to the lack of information concerning the exact provenance of the amber we do not constrain to precisely the age of taxa derivating from this deposit</p>
<p>Radiometric data established an early Cenomanian age (<math>98.79 \pm 0.62</math> Ma) while some ammonites found in the amber-bearing bed and within amber corroborate a late Albian / early Cenomanian age (Cruickshank &amp; Ko, 2003; Yu <i>et al.</i>, 2019). We use the minimum age recovered from zircon and a mid-Albian age allowing errors due to the older stratigraphic levels currently mined and where the amber pieces might have</p>
<p>Dominican amber is mined from several deposit dated from the Langhian-Burdigalian ( Iturralde-Vincent &amp; MacPhee, 1996; Seyfullah <i>et al.</i>, 2018). Due to the lack of information concerning the exact provenance of the amber we do not constrain to precisely the age of taxa derivating from this deposit</p>
<p>Dominican amber is mined from several deposit dated from the Langhian-Burdigalian ( Iturralde-Vincent &amp; MacPhee, 1996; Seyfullah <i>et al.</i>, 2018). Due to the lack of information concerning the exact provenance of the amber we do not constrain to precisely the age of taxa derivating from this deposit</p>
<p>Blue Earth Formation was dated as late Bartonian to Priabonian (upper Eocene, ca. 33.9–37.2 Ma) based on palynological data (Kosmoswska-Ceranowicz <i>et al.</i>, 1997; Aleksandrova &amp; Zaporozhets, 2008).</p>
<p>Blue Earth Formation was dated as late Bartonian to Priabonian (upper Eocene, ca. 33.9–37.2 Ma) based on palynological data (Kosmoswska-Ceranowicz <i>et al.</i>, 1997; Aleksandrova &amp; Zaporozhets, 2008).</p>
<p>Radiometric data established an early Cenomanian age (<math>98.79 \pm 0.62</math> Ma) while some ammonites found in the amber-bearing bed and within amber corroborate a late Albian / early Cenomanian age (Cruickshank &amp; Ko, 2003; Yu <i>et al.</i>, 2019). We use the minimum age recovered from zircon and a mid-Albian age allowing errors due to the older stratigraphic levels currently mined and where the amber pieces might have</p>
<p>Radiometric data established an early Cenomanian age (<math>98.79 \pm 0.62</math> Ma) while some ammonites found in the amber-bearing bed and within amber corroborate a late Albian / early Cenomanian age (Cruickshank &amp; Ko, 2003; Yu <i>et al.</i>, 2019). We use the minimum age recovered from zircon and a mid-Albian age allowing errors due to the older stratigraphic levels currently mined and where the amber pieces might have</p>
<p>Blue Earth Formation was dated as late Bartonian to Priabonian (upper Eocene, ca. 33.9–37.2 Ma) based on palynological data (Kosmoswska-Ceranowicz <i>et al.</i>, 1997; Aleksandrova &amp; Zaporozhets, 2008).</p>
<p>Blue Earth Formation was dated as late Bartonian to Priabonian (upper Eocene, ca. 33.9–37.2 Ma) based on palynological data (Kosmoswska-Ceranowicz <i>et al.</i>, 1997; Aleksandrova &amp; Zaporozhets, 2008).</p>
<p>Mexican amber-bearing strata extend from the Balumtun Sandstone of the lower Miocene to the La Quinta Formation of the upper Oligocene (Poinar &amp; Brown, 2002). A lower Miocene mid-Oligocene age has been proposed by Berggren &amp; Van Couvering, (1974) while a recent publication proposed a Serravallian-Burdigalian age (Seyfullah <i>et al.</i>, 2018). Therefore we chose a mean age corresponding to the</p>

<p>Radiometric data established an early Cenomanian age (<math>98.79 \pm 0.62</math> Ma) while some ammonites found in the amber-bearing bed and within amber corroborate a late Albian / early Cenomanian age (Cruickshank &amp; Ko, 2003; Yu <i>et al.</i>, 2019). We use the minimum age recovered from zircon and a mid-Albian age allowing errors due to the <del>older stratigraphic levels currently mined and where the amber pieces might have</del></p> <p>Blue Earth Formation was dated as late Bartonian to Priabonian (upper Eocene, ca. 33.9–37.2 Ma) based on palynological data (Kosmoswska-Ceranowicz <i>et al.</i>, 1997; Aleksandrova &amp; Zaporozhets, 2008).</p>
<p>Blue Earth Formation was dated as late Bartonian to Priabonian (upper Eocene, ca. 33.9–37.2 Ma) based on palynological data (Kosmoswska-Ceranowicz <i>et al.</i>, 1997; Aleksandrova &amp; Zaporozhets, 2008).</p>
<p>The fossils are preserved in sideritic mudstone from the upper insect bed in the mudstone interval below British Geological Survey Bed 5c which is present at the top of this pit and suggests an early Barremian age for this site (Batten, 2009, and see <del>detailed lithostratigraphical logs in Ross and Cook 1995</del>)</p>
<p>Radiometric data established an early Cenomanian age (<math>98.79 \pm 0.62</math> Ma) while some ammonites found in the amber-bearing bed and within amber corroborate a late Albian / early Cenomanian age (Cruickshank &amp; Ko, 2003; Yu <i>et al.</i>, 2019). We use the minimum age recovered from zircon and a mid-Albian age allowing errors due to the <del>older stratigraphic levels currently mined and where the amber pieces might have</del></p> <p>Blue Earth Formation was dated as late Bartonian to Priabonian (upper Eocene, ca. 33.9–37.2 Ma) based on palynological data (Kosmoswska-Ceranowicz <i>et al.</i>, 1997; Aleksandrova &amp; Zaporozhets, 2008).</p>
<p>Radiometric data established an early Cenomanian age (<math>98.79 \pm 0.62</math> Ma) while some ammonites found in the amber-bearing bed and within amber corroborate a late Albian / early Cenomanian age (Cruickshank &amp; Ko, 2003; Yu <i>et al.</i>, 2019). We use the minimum age recovered from zircon and a mid-Albian age allowing errors due to the <del>older stratigraphic levels currently mined and where the amber pieces might have</del></p> <p>Amber found in three intervals in the upper part of the Grès du Liban. Hammana is found in the upper interval, located between the Jezzianian above and the "Banc de Mrejatt" below. The "Banc de Mrejatt" includes one biostratigraphically significant benthic foraminifer: <i>Eopalarbitolina transiens</i> (Cherchi &amp; Schroeder, 1999), which is a zonal marker of the lower to upper Barremian transition according to Schroeder <i>et al.</i> (2010). Accordingly the "Banc de Mrejatt" is correlated to the transgression of sequence Ba3 of Clavel <i>et al.</i> (2007) and ascribed a late early Barremian age. The</p>
<p>Radiometric data established an early Cenomanian age (<math>98.79 \pm 0.62</math> Ma) while some ammonites found in the amber-bearing bed and within amber corroborate a late Albian / early Cenomanian age (Cruickshank &amp; Ko, 2003; Yu <i>et al.</i>, 2019). We use the minimum age recovered from zircon and a mid-Albian age allowing errors due to the <del>older stratigraphic levels currently mined and where the amber pieces might have</del></p>
<p>Radiometric data established an early Cenomanian age (<math>98.79 \pm 0.62</math> Ma) while some ammonites found in the amber-bearing bed and within amber corroborate a late Albian / early Cenomanian age (Cruickshank &amp; Ko, 2003; Yu <i>et al.</i>, 2019). We use the minimum age recovered from zircon and a mid-Albian age allowing errors due to the <del>older stratigraphic levels currently mined and where the amber pieces might have</del></p>
<p>Blue Earth Formation was dated as late Bartonian to Priabonian (upper Eocene, ca. 33.9–37.2 Ma) based on palynological data (Kosmoswska-Ceranowicz <i>et al.</i>, 1997; Aleksandrova &amp; Zaporozhets, 2008).</p>

Tableau 1

Aleksandrova, G.N. & Zaporozhets, N.I. (2008) Palynological characteristics of Upper Cretaceous and Paleogene deposits on the west of the Sambian Peninsula (Kaliningrad region), Part 2. <i>Stratigraphy and Geological Correlation</i> , 16, 528–539.
Batten, D.J. (2009) An unusual megaspore of uncertain systematic affinity from Lower Cretaceous deposits in south-east England and its biostratigraphic and palaeoenvironmental significance. <i>Grana</i> , 48, 270–280.
Berggren, W.A. & Van Couvering, J.A. (1974) The late Neogene. <i>Palaeogeography Palaeoclimatology and Palaeoecology</i> , 16, 1–216.
Brenner, G.J. (1967) Early angiosperm pollen differentiation in the Albian to Cenomanian deposits of Delaware (U.S.A.). <i>Review of Palaeobotany and Palynology</i> , 1, 219–227.
Cherchi, A. & Schroeder, R. (1999). <i>Montseciella</i> , a new orbitolinid genus (Foraminiferida) from the Uppermost Hauterivian – Early Barremian of SW Europe. <i>Treballs del Museu de Geologia de Barcelona</i> , 8, 5–23.
Christopher, R.A. (1979) Normapollens and triporate pollen assemblages from the Raritan and Magothy Formations (Upper Cretaceous) of New Jersey. <i>Palynology</i> , 3, 73–121.
Clavel, B., Charollais, J., Conrad, M., Jan du Chêne, R., Busnardo, R., Gardin, S., Erba, E., Schroeder, R., Cherchi, A., Decrouez, D., Granier, B., Sauvagnat, J. & Weidmann, M. (2007). Dating and progradation of the Urgonian limestone from the Swiss Jura to South-East France. <i>Zeitschrift der Deutschen Gesellschaft für Geowissenschaften, Stuttgart</i>
Cobban, W.A. & Kennedy, W.J. (1990) Upper Cenomanian ammonites from the Woodbridge Clay Member of the Raritan Formation in New Jersey. <i>Journal of Paleontology</i> , 64,
Cruikshank, R.D. & Ko, K. (2003) Geology of an amber locality in the Hukawng Valley, northern Myanmar. <i>Journal of Asian Earth Sciences</i> , 21, 441–455.
De Franceschi D. & De Ploëg G. (2003) Origine de l'ambre des faciès sparnaciens (Éocène inférieur) du Bassin de Paris : le bois de l'arbre producteur. <i>Geodiversitas</i> , 25,
Doyle, J.A. & Robbins, E.I. (1977) Angiosperm pollen donation of the continental Cretaceous of the Atlantic Coastal Plain and its application to deep wells in the Salisbury Embayment. <i>Palynology</i> , 1, 43–78.
Iturralde-Vincent, M.A. & MacPhee, R.D.E. (1996) Age and palaeogeographical origin of Dominican amber. <i>Science</i> , 273, 1850–1852.
Kosmoswska-Ceranowicz, B., Kohlman-Adamska, A. & Grabowska, I. (1997) Erste Ergebnisse zur Lithologie und Palynologie der Bernstein- führenden Sedimente im Tagebau Primorskoje. <i>Metalla</i> , 66, 5–17.
Maksoud, S., Azar, D., Granier, B. & Gêze, R. (2017) New data on the age of the Lower Cretaceous amber outcrops of Lebanon. <i>Palaeoworld</i> , 26, 331–338.
Poinar, G. & Brown, A. (2002) <i>Hymenaea mexicana</i> sp. nov. (Leguminosae: Caesalpinioideae) from Mexican amber indicates Old World connections. <i>Botanical Journal of the Linnean Society</i> , 139, 125–132.
Pons, D., Berthou, P.-Y. & Campos, D.A. (1991) Quelques observations sur la palynologie de l'Aptien supérieur et de l'Albien du bassin d'Araripe (N.E. du Brésil). In: Campos, D.A., Vianna, M.S.S., Brito, P.M., Beurlen, G. (Eds), Atas do I simposio sobre a Bacia do Araripe e Bacias Interiores do Nordeste, Crato, pp. 241–252.
Rasnitsyn, A.P., Jarzembowski, E.A. & Ross, A.J. (1998) Wasps (Insecta: Vespida = Hymenoptera) from the Purbeck and Wealden (Lower Cretaceous) of southern England and their biostratigraphical and palaeoenvironmental significance. <i>Cretaceous Research</i> , 19, 329–391.
Ross, A.J. & Cook, E. (1995) The stratigraphy and palaeontology of the Upper Weald Clay (Barremian) at Smokejacks Brickworks, Ockley, Surrey, England. <i>Cretaceous</i>
Schroeder, R., van Buchem, F.S.P., Cherchi, A., Baghbani, D., Vincent, B., Immenhauser, A. & Granier, B. (2010) Revised orbitolinid biostratigraphic zonation for the Barremian – Aptian of the eastern Arabian Plate and implications for regional stratigraphic correlations. <i>GeoArabia Special Publication 4</i> , 49–96.
Seyfullah, L.J., Beimforde, C., Dal Corso, J., Perrichot, V., Rikkinen, J. & Schmidt, A.R. (2018) Production and preservation of resins – past and present. <i>Biological Reviews</i> , 93,
Shi, G.H., Grimaldi, D.A., Harlow, G.E., Wang, J., Wang, J., Yang, M.C., Lei, W.Y., Li, Q.L. & Li, X.H. (2012) Age constraint on Burmese amber based on U-Pb dating of zircons. <i>Cretaceous Research</i> , 37, 155–163.
Vakhrameev, V.A. & Kotova, I.Z. (1977) Ancient angiosperms and associated plants from the Lower Cretaceous deposits of Transbaikalia. <i>Paleontologicheskii Zhurnal</i> , 4,
Yu, T., Kelly, R., Mu, L., Ross, A., Kennedy, J., Broly, P., Xia, F., Zhang, H., Wang, B. & Dölicher, D. (2019) An ammonite trapped in Burmese amber. <i>Proceedings of the National Academy of Sciences of the United States of America</i> , 116, 11345–11350.

Run	# partitions	Prior ingroup	method	fossil calibration	sampling
ND	1 offsetexp(137,150)	<b>Node dating</b>	NA	diversity	
ND-BD-random	1 offsetexp(137,150)	<b>Node dating</b>	NA	random	
ND-uni-random	1 offsetexp(137,150)	<b>Node dating</b>	NA	random	
ND-uni-diversity	1 offsetexp(137,150)	<b>Node dating</b>	NA	diversity	
1p	1 offsetexp(137,150)	Tip dating	uniform	fossiltip (noSA)	
1p - 144	1 <b>offsetexp(137,144)</b>	Tip dating	uniform	fossiltip (noSA)	
1p - 163	1 <b>offsetexp(137,163)</b>	Tip dating	uniform	fossiltip (noSA)	
3p	3 offsetexp(137,150)	Tip dating	uniform	fossiltip (noSA)	
3p rate variable	3 offsetexp(137,150)	Tip dating	uniform	fossiltip (noSA)	
1p-equal	1 offsetexp(137,150)	Tip dating	uniform	fossiltip (noSA)	
1p-flatpriors	1 offsetexp(137,150)	Tip dating	uniform	fossiltip (noSA)	
1p-fixed-diversity	1 offsetexp(137,150)	Tip dating	<b>fixed</b>	<b>diversity</b>	
1p-fixed-fossiltip	1 offsetexp(137,150)	Tip dating	<b>fixed</b>	fossiltip (noSA)	
1p-fixed-random	1 offsetexp(137,150)	Tip dating	<b>fixed</b>	<b>random</b>	
1p-uni-diversity	1 offsetexp(137,150)	Tip dating	uniform	<b>diversity</b>	
1p-uni-random	1 offsetexp(137,150)	Tip dating	uniform	<b>random</b>	
1p-clock_uni	1 offsetexp(137,150)	Tip dating	uniform	fossiltip (noSA)	

	Tree prior	Model	Relative rate setting for morphology partition	Tree age prior	Estimated root age (in my)	95%HPD root age
birthdeath	Mkv + G	fixed	offsetexp(225,270)	240.6735	225.0008 - 284.9263	
birthdeath	Mkv + G	fixed	offsetexp(225,270)	238.9243	225.0005 - 279.7332	
uniform	Mkv + G	fixed	offsetexp(225,270)	258.5857	225.0034 - 333.5385	
uniform	Mkv + G	fixed	offsetexp(225,270)	258.446	225.0008 - 336.6207	
fossilization (BDSS)	Mkv + G	fixed	offsetexp(225,270)	243.6179	225.0006 - 283.5012	
fossilization (BDSS)	Mkv + G	fixed	offsetexp(225,270)	237.688	225.003 - 272.0503	
fossilization (BDSS)	Mkv + G	fixed	offsetexp(225,270)	246.3578	225.0032 - 291.2503	
fossilization (BDSS)	Mkv + G	fixed	offsetexp(225,270)	249.8804	225.0005 - 296.9502	
fossilization (BDSS)	Mkv + G	<b>variable</b>	offsetexp(225,270)	251.2182	225.0256 - 294.8504	
fossilization (BDSS)	<b>Mkv</b>	fixed	offsetexp(225,270)	243.45	225.0004 - 280.0379	
fossilization (BDSS)	Mkv + G	fixed	offsetexp(225,270)	244.2911	225.0072 - 281.5017	
fossilization (BDSS)	Mkv + G	fixed	offsetexp(225,270)	229.31.81	225.0009 - 242.8222	
fossilization (BDSS)	Mkv + G	fixed	offsetexp(225,270)	241.9179	225.0015 - 279.3208	
fossilization (BDSS)	Mkv + G	fixed	offsetexp(225,270)	286.8833	238.9085 - 343.6958	
fossilization (BDSS)	Mkv + G	fixed	offsetexp(225,270)	282.6479	234.7861 - 331.6037	
fossilization (BDSS)	Mkv + G	fixed	offsetexp(225,270)	307.0385	254.2658 - 364.2134	
<b>uniform</b>	Mkv + G	fixed	offsetexp(225,270)	335.8605	240.03 - 448.769	

SD split frequencies	arithmetic mean marginal LnL	harmonic mean marginal LnL	Average ESS for TL	Clock Rate Prior	Mean estimated clock rate	95%HPD of estimated clock rate	Relaxed clock model
0.003347	-1017.45	-1073.01	3844.99	gamma (2,200)	0.001084	0.000552 - 0.001673	IGR
0.002992	-1018.94	-1074.07	3465.77	gamma (2,200)	0.001103	0.000568 - 0.001722	IGR
0.003359	-1015.27	-1061.35	4333.46	gamma (2,200)	0.000750	0.000426 - 0.001114	IGR
0.002953	-1015.97	-1060.75	4730.44	gamma (2,200)	0.000748	0.000425 - 0.001110	IGR
0.005948	-1652.89	-1726.05	3041.98	gamma (2,200)	0.001468	0.000968 - 0.002038	IGR
0.004800	-1655.68	-1735.25	3351.94	gamma (2,200)	0.001526	0.000985 - 0.002088	IGR
0.005522	-1655.21	-1730.83	3611.75	gamma (2,200)	0.001434	0.000924 - 0.001979	IGR
0.007870	-1638.53	-1729.58	2052.92	gamma (2,200)	0.001447	0.000959 - 0.001965	IGR
0.006890	-1643.08	-1726.95	2436.13	gamma (2,200)	0.001524	0.000984 - 0.002120	IGR
0.006027	-1695.03	-1769.22	2352.46	gamma (2,200)	0.001215	0.000938 - 0.001500	IGR
0.005028	-1654.29	-1725.98	3540.81	<b>normal(0.0025,1)</b>	0.001427	0.000944 - 0.001975	IGR
0.005025	-1781.23	-1838.72	2280.86	gamma (2,200)	0.003034	0.002167 - 0.003995	IGR
0.004831	-1648.80	-1734.16	3462.06	gamma (2,200)	0.001498	0.000980 - 0.002054	IGR
0.005033	-1740.29	-1801.50	2012.46	gamma (2,200)	0.001586	0.001092 - 0.002088	IGR
0.004945	-1750.22	-1807.29	1330.00	gamma (2,200)	0.001564	0.001099 - 0.002059	IGR
0.004066	-1744.75	-1798.99	1619.54	gamma (2,200)	0.001508	0.001046 - 0.001991	IGR
0.005301	-1650.89	-1728.98	2773.18	gamma (2,200)	0.000921	0.000571 - 0.001291	IGR

---

<b>Prior on variance of branch rate variability (relaxed clock)</b>	<b>Estimated mean of branch rate variance parameter</b>
exp(10) 0.025828	
exp(10) 0.021394	
exp(10) 0.034740	
exp(10) 0.034663	
exp(10) 0.033491	
exp(10) 0.034390	
exp(10) 0.033085	
exp(10) 0.033833 / 0.010602 / 0.010236	
exp(10) 0.035823 / 0.011856 / 0.010189	
exp(10) 0.026827	
exp(10) 0.033030	
exp(10) 0.000015	
exp(10) 0.032651	
exp(10) 0.000002	
exp(10) 0.000003	
exp(10) 0.000002	
exp(10) 0.042635	

---

95%HPD estimated mean of branch rate variance parameter	Speciation prior	Mean estimated net speciation
0.008587 - 0.047045	exp(100)	0.005728
0.005484 - 0.040812	exp(100)	0.010152
0.014192 - 0.058913	exp(100)	NA
0.014179 - 0.059021	exp(100)	NA
0.016177 - 0.053074	exp(100)	0.010941
0.016517 - 0.053965	exp(100)	0.011249
0.016062 - 0.052708	exp(100)	0.010853
0.017355 - 0.052489 / 0.000158 - 0.023042 / 0.000427 - 0.024153	exp(100)	0.010456
0.017128 - 0.055651 / 0.000866 - 0.026291 / 0.000160 - 0.024042	exp(100)	0.010502
0.014452 - 0.040579	exp(100)	0.011098
0.016564 - 0.052536	<b>uniform (0,10)</b>	0.012143
0.000001 - 0.000072	exp(100)	0.006583
0.015751 - 0.051603	exp(100)	0.011270
0.000001 - 0.000005	exp(100)	0.007775
0.000001 - 0.000008	exp(100)	0.004947
0.000001 - 0.000004	exp(100)	0.007455
0.022218 - 0.065331	exp(100)	NA

	<b>Mean estimated relative extinction</b>	<b>Mean estimated relative fossilization</b>	<b>Mean estimated prop ancossil</b>	<b>mean estimated alpha</b>
0.999044	NA	NA	0.761095	
0.994413	NA	NA	0.770354	
NA	NA	NA	0.788574	
NA	NA	NA	0.782024	
0.990651	0.000146	NA	1.000262	
0.990955	0.000141	NA	0.993476	
0.990554	0.000146	NA	1.002776	
0.991736	0.000128	NA	1.010478	
0.991702	0.000129	NA	0.989421	
0.989654	0.000161	NA	NA	
0.989273	0.000157	NA	0.994736	
0.999815	0.000001	0.000588	0.989939	
0.990661	0.000145	NA	0.993981	
0.995851	0.000061	0.000868	1.076293	
0.999339	0.000005	0.000636	1.098813	
0.995690	0.000063	0.001081	1.074011	
NA	NA	NA	1.065258	

**List of the 17 analyses computed in 'Revising dating estimates and the antiquity of eusociality in termites using the fossilized birth-death process'**

ND: node dating analysis with a birth-death tree prior; one partition; diversity sampling

ND-BD-random: same as ND but with a random sampling

ND-uni-diversity: node dating analysis with a uniform tree prior; one partition; diversity sampling

ND-uni-random: same as ND-uni-diversity but with a random sampling

1p-clock uni: tip-dating analysis with a uniform clock tree prior; one partition, uniform fossil calibrations

1p: tip-dating analysis with a birth-death serial sampling (i.e. no sampled ancestor); one partition; uniform fossil calibrations

1p halved: same as 1p but with a more restricted age prior for the ingroup

1p twice: same as 1p but with an extended age prior for the ingroup

3p: same as 1p but with three partitions

3p rate variable: same as 3p but with a variable relative rate setting for partitions

1p-equal: same as 1p but with a Mkv model (and not a Mkv + G)

1p-uni-diversity: same as 1p but with a diversity sampling (sampled ancestor allowed)

1p-uni-random: same as 1p but with a random sampling (sampled ancestor allowed)

1p-flatpriors: same as 1p but with flat clock rate and speciation priors

1p-fixed-fossiltip: same as 1p but with fixed fossil calibrations

1p-fixed-diversity: same as 1p but with fixed fossil calibrations and a diversity sampling (sampled ancestor allowed)

1p-fixed-random: same as 1p but with fixed fossil calibrations and a random sampling (sampled ancestor allowed)

**List of the 17 analyses computed in 'Revising dating estimates and the antiquity of eusociality in termites using the fossilized birth-death process'**

ND: node dating analysis with a birth-death tree prior; one partition; diversity sampling

ND-BD-random: same as ND but with a random sampling

ND-uni-diversity: node dating analysis with a uniform tree prior; one partition; diversity sampling

ND-uni-random: same as ND-uni-diversity but with a random sampling

1p-clock uni: tip-dating analysis with a uniform clock tree prior; one partition, uniform fossil calibrations

1p: tip-dating analysis with a birth-death serial sampling (i.e. no sampled ancestor); one partition; uniform fossil calibrations

1p halved: same as 1p but with a more restricted age prior for the ingroup

1p twice: same as 1p but with an extended age prior for the ingroup

3p: same as 1p but with three partitions

3p rate variable: same as 3p but with a variable relative rate setting for partitions

1p-equal: same as 1p but with a Mkv model (and not a Mkv + G)

1p-uni-diversity: same as 1p but with a diversity sampling (sampled ancestor allowed)

1p-uni-random: same as 1p but with a random sampling (sampled ancestor allowed)

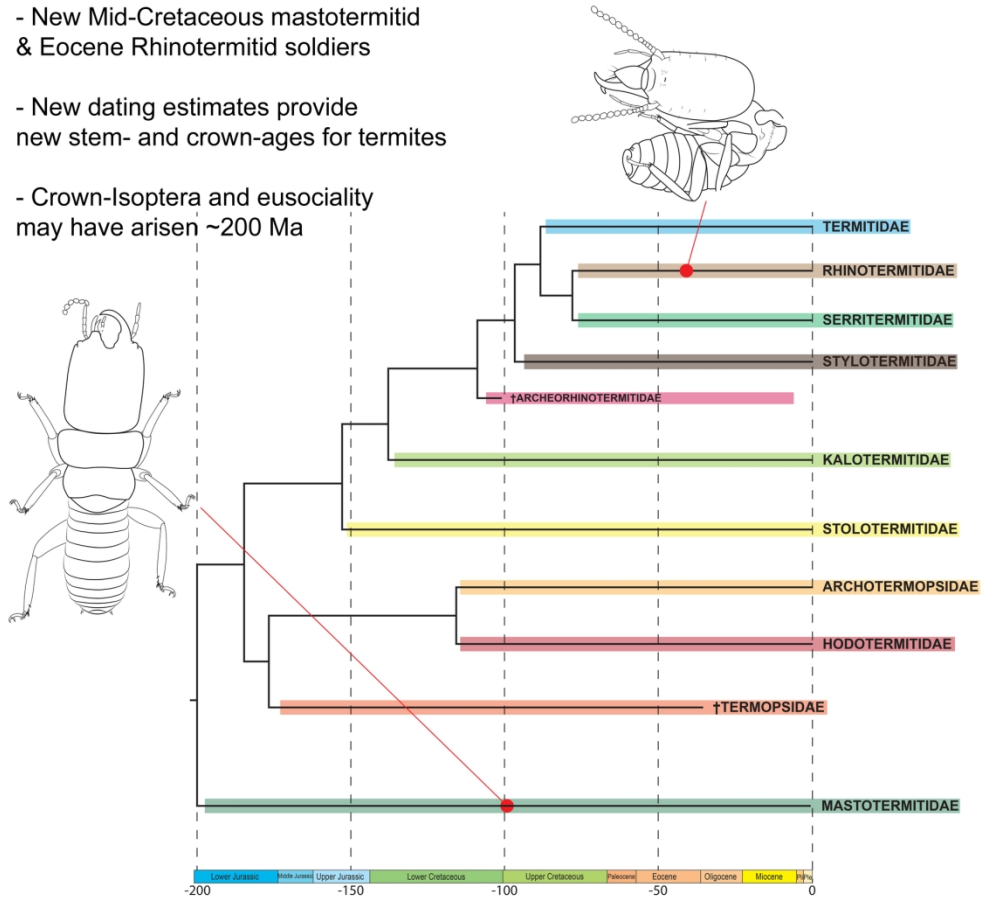
1p-flatpriors: same as 1p but with flat clock rate and speciation priors

1p-fixed-fossiltip: same as 1p but with fixed fossil calibrations

1p-fixed-diversity: same as 1p but with fixed fossil calibrations and a diversity sampling (sampled ancestor allowed)

1p-fixed-random: same as 1p but with fixed fossil calibrations and a random sampling (sampled ancestor allowed)

- New Mid-Cretaceous mastotermitid & Eocene Rhinotermitid soldiers
- New dating estimates provide new stem- and crown-ages for termites
- Crown-Isoptera and eusociality may have arisen ~200 Ma



graphical abstract

169x152mm (300 x 300 DPI)

Revising dating estimates and the antiquity of eusociality in termites using the fossilized birth-death process

CORENTIN JOUAULT<sup>\*,1, †</sup>, FREDERIC LEGENDRE<sup>2, †</sup>, PHILIPPE GRANDCOLAS<sup>2</sup> and ANDRE NEL<sup>\*,2</sup>

\*Corresponding authors

† Equal contributions

### Highlights

New Mid-Cretaceous mastotermitid & Eocene Rhinotermitid soldiers

New dating estimates provide new stem- and crown-ages for termites

Crown-Isoptera and eusociality may have arisen ~200 Ma